Temporal and Notch identity determine layer targeting and synapse location of medulla neurons

Holguera, I.[1,2], Chen Y-C. [1], Chen Y-C-D.[1], Simon F. [1,2], Gaffney A.G. [1], Rodas J.D.[1], Córdoba S. [1], and Desplan C.[1,3]*.*

[1]Department of Biology, New York University, New York, NY 10003, USA.

[2]Current address: Institut Jacques Monod, Centre National de la Recherche Scientifique-UMR7592-Université Paris Cité, Paris, France

[3]Center for Genomics and Systems Biology, New York University Abu Dhabi, Abu Dhabi, United Arab Emirates.

* Correspondence: isabel-maria.holguera-lopez@ijm.fr, cd38@nyu.edu

Abstract

How specification mechanisms that generate neural diversity translate into specific neuronal targeting, connectivity, and function in the adult brain is not understood. In the medulla region of the *Drosophila* optic lobe, neural progenitors generate different neurons in a fixed order by sequentially expressing a series of temporal transcription factors as they age. Then, Notch signaling in intermediate progenitors further diversifies neuronal progeny. By establishing the birth order of medulla neurons, we found that their temporal identity correlates with the depth of neuropil targeting in the adult brain, for both local interneurons and projection neurons. We show that this temporal identity-dependent targeting of projection neurons unfolds early in development and is genetically determined. By leveraging the Electron Microscopy reconstruction of the adult fly brain, we determined the synapse location of medulla neurons in the different optic lobe neuropils and find that it is significantly associated with both their temporal identity and Notch status. Moreover, we show that all the putative medulla neurons with the same predicted function share similar neuropil synapse location, indicating that ensembles of neuropil layers encode specific visual functions. In conclusion, we show that temporal identity and Notch status of medulla neurons can predict their neuropil synapse location and visual function, linking their developmental patterning with their specific connectivity and functional features in the adult brain.

Introduction

The brain is comprised of thousands of different neuronal types with distinct morphologies and functions that form precise neural networks during development to control specific behaviors. Much progress has been made in elucidating the mechanisms that give rise to this neural diversity, both in vertebrates and invertebrates[1-2]. In both systems spatial patterning first diversifies the progenitor pool based on the expression of specific spatial transcription factors (TFs) and signaling molecules[3-5]. Then, neural stem cells emerging from these spatial regions change their competence over time to produce different neurons based on the expression of cascades of temporal TFs (tTFs)[6-12] or RNA-binding protein gradients in flies[13-14], or the temporal expression of different TF modules in mammals[15-18]. Moreover, in invertebrates, a Notch-dependent binary cell fate decision at the level of an intermediate progenitor (called Ganglion Mother Cell or GMC) further diversifies the neuronal progeny, giving rise to two neurons, one where Notch signaling is active ($Notch^{On}$), and one where Notch signaling is inactive ($Notch^{Off}$)[7, 19-21]. A similar mechanism has been shown

in vertebrates[22-24], although the role that Notch plays in diversifying neuronal progeny in vertebrate systems is much less studied. How these patterning mechanisms either individually or in conjunction, impact circuit connectivity is not well understood.

One of the neural structures best characterized in terms of the developmental principles that give rise to its cellular diversity is the main Outer Proliferation Center (main OPC) within the *Drosophila* optic lobe, the region that produces most neurons of the medulla (see below). Single cell RNA sequencing (scRNA-seq) approaches at neurogenesis stages have allowed the comprehensive characterization of the tTFs that pattern main OPC neural stem cells (called neuroblasts or NBs in *Drosophila*), as well as the spatial origin and the relative birth order of all the neurons produced in this region[11-12,25] (**Fig. 1A**). This also allowed the identification of the Notch status of all the main OPC neurons, based on the expression of the TF Apterous, a marker of Notch^{On} neurons[7,11]. Notch^{On} and Notch^{Off} neurons in the main OPC have different morphology and neurotransmitter identity[11]. In the *Drosophila* Ventral Nerve Cord (VNC) hemilineages (all the Notch^{On} or Notch^{Off} progeny from a given NB) share the expression of specific TFs and common synaptic targeting within the neuropil[21,26-27]. Moreover, hemilineage temporal cohorts share common connectivity[21]. However, a comprehensive analysis of how temporal patterning and Notch status are associated with neuronal targeting, connectivity and function in the optic lobe was lacking.

The optic lobe is comprised by four different highly interconnected ganglia: the lamina, medulla, lobula, and lobula plate. These ganglia are composed of a neuronal cortex, where neuronal somas reside, and a neuropil, where the neurites of the neurons from the same or different ganglia project to form connections[28]. Neurons in the main OPC can be broadly divided in two classes: local interneurons (neurons that arborize exclusively in the medulla), such as Proximal medulla (Pm), Distal medulla (Dm), Serpentine medulla (Sm), and Medulla intrinsic (Mi) neurons; projection neurons (neurons that target both the medulla neuropil and at least one additional neuropil), such as Transmedullary (Tm), Transmedullary Y (TmY), two Lobula intrinsic (Li), and T1 neurons[29-30] (**Fig. 1B**). We and others have previously generated a transcriptomic atlas of the cellular diversity of the optic lobe from neurogenesis to adult stages, identifying 172 distinct neuronal and 19 glial clusters[31-33]. Out of the 172 neuronal types (clusters), 103 are generated from the main OPC[11] (**Fig 1C**). From these, Notch^{On} neurons are generally projection neurons of cholinergic identity, while Notch^{Off} neurons are usually inhibitory interneurons, which are most often either glutamatergic or GABAergic[11] (**Fig. 1C**). Within each of these neuronal classes, further subdivisions (i.e. morphological types) are based on distinct arborization patterns and projections to different layers within the neuropil(s)[29,34-36]. The segregation of neuronal processes into different layers is a common organization principle in very different neural structures, such as the *Drosophila* ellipsoid body, the vertebrate optic tectum, and the mammalian cortex and retina[37-39]. This lamination segregates specific connections between synaptic partners in a restricted space, potentially making easier the process of axon navigation and connectivity. However, how these layers and specific wiring patterns arise during development is not well understood. Although an extensive body of work has focused on understanding late stages of circuit formation such as synaptic partner matching[40-41], the influence that earlier developmental processes such as neuronal specification programs in progenitors have on connectivity has been less studied. The comprehensive description of main OPC neural diversity at single-cell resolution, the detailed understanding of the specification programs that give rise to this diversity in a stereotyped order, and the recently completed Electron Microscopy (EM) reconstruction (connectome) of the adult fly brain, which provides a complete catalog of all the optic lobe morphological diversity and their

connectivity at synapse resolution[30,42-43], make this system ideal to understand the link between developmental programs and connectivity.

Here we analyze how shared temporal origin and Notch identity of main OPC neurons impact the depth of neuropil targeting, connectivity, and function. For this, we leveraged the connectome of the adult fly brain (FlyWire dataset) [30,42] and identified the neuropil layers at which main OPC neurons terminate, and the location of their synaptic inputs and outputs within the different optic lobe neuropils. We found that local interneurons as well as projection neurons target different neuropil layers depending on their temporal identity and Notch status: earlier born interneurons target the Proximal medulla, while later born interneurons target the Distal medulla. Early born Notch^{On} projection neurons target superficial layers of the lobula, while later born Notch^{On} projection neurons target deep layers. Interestingly, Notch^{Off} projection neurons do not display a noticeable birth order-associated targeting pattern. Moreover, we show that temporal identity of main OPC neurons predicts neuropil targeting depth and synapse location in both the medulla and lobula. Furthermore, by leveraging functional models inferred from connectivity in FlyWire, we show that different visual functions are significantly associated with specific temporal origins and groups of neuropil layers. Notably, using synapse location of all the putative main OPC neurons, we can predict their temporal origin, linking their connectivity with their developmental programs. Altogether, these results provide a link between temporal identity, connectivity, and function in the largest and most diverse neuropil of the optic lobe, highlighting the role of specification programs to set an initial plan of the brain circuits that compose the adult brain.

Results

Link between temporal identity and depth of neuropil targeting of main OPC neurons

Main OPC neurons are generated in a specific order by temporal patterning of their progenitors[7-8,11-12]. During neurogenesis, newly born neurons displace earlier born neurons away from the parent NB, creating a columnar arrangement of neuronal somas where early born neurons are located closer to the emerging medulla neuropil and later born neurons are located further away[11,44] (**Fig. 1A**). Leveraging this feature of main OPC neurons and their specific expression of combinations of TFs[11,44], we recently determined the relative temporal identity of ~100 main OPC neurons corresponding to scRNA-seq clusters and assigned them to eight broad temporal windows[11]. Forty-six of these clusters have been annotated as corresponding to known neurons[32-33,45-46] (**Fig. 1C**).

The specific morphology of main OPC neurons results in part from the specific regions (layers) of the different neuropils at which the neurites of these neurons arborize. To determine whether the temporal origin of main OPC neurons is associated with neuropil targeting depth, we examined the specific neuropil targeted and the layers within the neuropil at which these neurons terminate in the adult. At this stage, the medulla neuropil is comprised by 10 different layers (M1-M10), and it can be subdivided in the Proximal medulla (M8-M10) and the Distal Medulla (M1-M6), which are separated by a layer of tangential fibers called the Serpentine layer (M7)[28-29] (**Fig. 1B**). The lobula is comprised by six different layers (Lo1-Lo6) in the adult. In this work we subdivide the lobula in superficial layers (Lo1-Lo4) and deep layers (Lo5-Lo6), with each group accounting for ~50% of the neuropil volume[28-29] (**Fig. 1B**). We analyzed neuropil targeting depth of known (annotated) main OPC interneurons and projection neurons independently, since interneurons remain in the medulla while projection neurons terminate in the lobula (**Fig. 1B**).

- Interneurons: All main OPC interneurons are Notch^{Off} (Ap^{-}), except Mi1 and Mi10 (**Supp. Fig. 1A**). All the annotated Pm (Pm1-Pm4) and Mi neurons (Mi1, Mi4, Mi9 and Mi10) are born within the first four temporal windows and all terminate in the Proximal medulla. Moreover, all the annotated Dm interneurons, which target the Distal medulla, are born later, from the 5th temporal window onwards[5,11] (**Fig. 1D**). Furthermore, Mi15, which projects to the Serpentine layer and it is the only annotated Sm neuron (see Methods), is born in the last (8th) temporal window (**Fig. 1D**).

- Projection neurons: All the annotated Notch^{On} projection neurons born within the first five temporal windows terminate within superficial layers of the lobula (Lo1 to Lo4), while projection neurons born later terminate at deeper lobula layers (Lo5-Lo6) (**Figure 1E**). In the case of Notch^{Off} projection neurons (six out of 19) (**Supp. Fig. 1A**), the ones targeting superficial layers of the lobula are born in the first (Li14, TmY15) and sixth (TmY14, which also targets the central brain) temporal windows, while the ones targeting deep lobula layers (Lo5-Lo6) are born in the 3rd and 4rd temporal windows, indicating that Notch^{Off} projection neurons do not display a noticeable birth order-associated targeting pattern.

Next, we tested whether the correlation between temporal origin and lobula layer targeting depth of main OPC Notch^{On} projection neurons, where neurons born late target deep lobula layers, held true for most of the remaining projection neurons. If late born projection neurons terminate within deep layers of the lobula (Lo5-Lo6), then stopping the temporal cascade before late temporal windows (and hence not producing late born neurons) would generate projection neurons only targeting the superficial layers of the lobula (Lo1-Lo4). We stopped the temporal cascade at a late temporal window by generating NB MARCM *slp* mutant clones[47]. In wild-type NB clones all six lobula layers were innervated (**Fig. 1F**). However, in *slp* mutant clones, there was a 1.5-fold reduction in the innervation of the deepest layers of the lobula neuropil (Lo5-Lo6) (**Fig. 1G-H; Supp. Table 1**), indicating that projection neurons that target deep layers of the lobula are usually generated either within the Slp expression window or after. It is worth mentioning that, apart from neurons generated from the main OPC, the lobula neuropil is additionally targeted by neurons from other origins, such as the central brain, the Inner Proliferation Center (IPC), and the tips of the OPC (tOPC), which could also be affected by the *slp* mutation. Therefore, these results indicate that most of the main OPC projection neurons targeting deep layers of the lobula neuropil are generated in late temporal windows.

Lobula layer targeting of main OPC projection neurons is established early

Since we uncovered a correlation between the temporal identity of Notch^{On} projection neurons and lobula neuropil targeting depth, where early born neurons target superficial layers and late born neurons target deeper layers (**Fig. 1E-H**), we next sought to determine when this segregation occurs during development. The adult lobula layers develop from protolayers, which are broader targeting regions that are progressively refined as the neurites from different neurons segregate with time[28]. We performed double labelling of early born Notch^{On}, either Tm9 (terminates at Lo1 in the adult) or Tm3 (terminates at Lo4 in the adult) neurons, and late born Notch^{On} Tm25 neurons (terminates at Lo5 in the adult) (**Fig. 1E**) and followed their axon targeting process by immunostaining at different stages throughout development. **Fig. 2** shows that both Tm9 and Tm3 neurons target a more superficial protolayer than Tm25 neurons throughout development. At 15h after puparium formation (APF), the axons of both the early and the late born neurons are very close to each other in the lobula, although they are already segregated, with Tm25 targeting deeper (**Fig. 2A-A'**). At this stage, the exploratory region of both Tm9 and Tm3 growth

cones is broad, probably encompassing half of the lobula neuropil (**Fig. 2A-A'**). At 24h APF, the distance between the neurites of Tm9 and Tm25 increases, with the axons of Tm9 being more restricted to the most superficial protolayer (**Fig. 2B**). At this stage, the neurites of Tm3 and Tm25 remain close, although clearly targeting different protolayers, with Tm25 targeting deeper (**Fig. 2B'**). At 48h APF, the final six layers of the adult lobula can already be identified[28], and Tm9 axons are restricted to the Lo1 layer, while Tm3 arbors at Lo2 and Lo4 are clearly segregated, and Tm25 axons occupy Lo5 (**Fig. 2C-C'**). Hence, the superficial targeting of the early born Tm9 and Tm3 neurons and the deep targeting of the late born Tm25 neuron is established at early stages, and their neurites progressively segregate from each other as development proceeds.

Neuropil synapse location of main OPC neurons is associated with their specific temporal origins

Most neural processes in fly neurons carry a combination of presynapses and postsynapses[42,48-49]. We sought to determine whether synapse location of main OPC neurons was associated with their specific temporal origins. We thus mapped both the presynapses and postsynapses of main OPC neurons from different temporal origins in the medulla, lobula, and lobula plate neuropils using neuronal type-specific synaptic coordinates from the FlyWire dataset[30,42] (codex.FlyWire.ai; see Methods) (**Fig. 3**). We separated Notch^{On} from Notch^{Off} neurons, as these neurons are very different from each other, with most of the Notch^{On} being projection neurons and most of the Notch^{Off} being interneurons (**Supp. Fig. 1A-B**).

- The medulla neuropil contains all the inputs and outputs from main OPC interneurons. Synapse location of Notch^{Off} neurons in the medulla was significantly associated with their temporal identity, both in the case of presynapses and postsynapses (**Fig. 3A-A'; Supp. Table 1**). For example, both pre and postsynapses of Notch^{Off} neurons from the first (Hth) temporal window were enriched in the Proximal medulla, while pre and postsynapses of Notch^{Off} neurons from later temporal windows (Ey/Hbn/Opa, Slp/D, and D/BarH1) were enriched in the Distal medulla. Notch^{Off} neurons from the fourth (Erm/Ey) temporal window (which are projection neurons) have both pre and postsynapses enriched in and around the Serpentine layer (**Fig. 3A-A'**).

In the case of Notch^{On} neurons, which comprise most of the main OPC projection neurons, postsynapses of neurons from all the temporal windows are enriched in the Distal medulla, where some of them receive inputs from R7 and R8 color photoreceptors and from lamina neurons L1-L5. Only presynapses of neurons from the late sixth and seventh (Hbn/Opa/Slp and Slp/D) temporal windows are enriched in the Distal medulla, while presynapses of neurons from the rest of the temporal windows are enriched in the Proximal medulla (**Fig. 3B-B'**).

- The lobula neuropil contains most of the presynaptic inputs of main OPC projection neurons (Tms, TmYs, Li06 and Li14). Both pre- and postsynapses of Notch^{On} neurons from the earlier temporal windows (Hth/Opa, Erm/Ey, Ey/Hbn/Opa) were enriched in the superficial layers (Lo1-Lo4), while pre- and postsynapses of neurons from later temporal windows (Hbn/Opa/Slp and Slp/D) were enriched in deeper layers (**Fig. 3C-C'**).

On the other hand, although both pre- and postsynapses of Notch^{Off} projection neurons from the first (Hth) temporal window were enriched in the superficial lobula (Lo1-Lo4), both pre- and postsynapses of Notch^{Off} neurons from the third and fourth (Opa/Erm and Erm/Ey) windows (i.e., Tm5c, Tm5d and TmY5a) were enriched in deep lobula layers (Lo5-Lo6) (**Fig. 3D-D'**), in agreement with the termination of these neurons in these layers described above (**Fig. 1E**). Moreover, both pre- and postsynapses of Notch^{Off} TmY14 neurons (sixth temporal window, Hbn/Opa/Slp) were enriched in the superficial lobula (**Fig. 3D-D'**). These results indicate that

Notch^{Off} projection neurons do not display a noticeable birth order-associated targeting pattern, as is the case of Notch^{On} projection neurons.

Within the annotated main OPC projection neurons, TmYs are the only neurons that also target the lobula plate (Lop1-Lop4). In this neuropil, the location of only postsynapses of Notch^{Off} neurons between the first (Hth), and the fourth (Erm/Ey) and sixth (Hbn/Opa/Slp) temporal windows (**Supp. Fig. 2A-B'; Supp. Table 1**) was significantly different, which could indicate either that synapse location is not strongly associated with temporal origin of main OPC neurons in the lobula plate or that there are not enough annotated neurons that target this neuropil to see this association.

In summary, our data shows that there is a significant association between the specific temporal origins of main OPC neurons and their synapse location in both the medulla and lobula neuropils, both for their presynapses and postsynapses.

Temporal identity of main OPC neurons predicts their neuropil targeting depth and synapse location

Since we uncovered a significant association between temporal identity and both neuropil targeting depth and synapse location of known main OPC neurons, we next asked whether neurons for which we did not know their identity (unannotated clusters) share the same neuropil termination depth and synapse location than known main OPC neurons from the same temporal origin. We chose to investigate the morphological identity of neurons generated in the sixth (Hbn/Opa/Slp) and eigth (D/BarH1) temporal windows, hypothesizing that Notch^{On} neurons would be projection neurons targeting deep lobula layers, and Notch^{Off} neurons would be interneurons targeting the Distal medulla, as was the case for the known annotated neurons (see **Fig. 1D-E and Fig. 3A-A', C-C'**). Moreover, we also characterized the unannotated Notch^{Off} neurons generated in the fourth (Erm/Ey) temporal window, hypothesizing that if they were projection neurons, they would also target deep layers of the lobula, like their known counterparts (see **Fig. 1E and Fig. 3D-D'**).

The Hbn/Opa/Slp temporal window contains 12 unannotated clusters, of which clusters 45, 52, 53, 59, 69, 82, 88a, 88b, and 103 are Notch^{On} (Ap+) and cholinergic, and clusters 11, 38, and 39 are Notch^{Off} and glutamatergic[11] (**Supp. Fig. 3A)**. To identify the morphology of the neurons that correspond to these clusters, we built specific split-Gal4 drivers based on the co-expression of gene pairs in each cluster in the adult informed from the scRNA-seq dataset, as previously described[46,50]. We built split-Gal4 lines to label 8 out of these 12 clusters in the adult brain: 38, 39, 45, 52, 53, 59, 69 and 82 and used them to drive UAS-myristoylated (myr) GFP (**Supp. Fig. 4A-H**), and MultiColor FlpOut (MCFO)[36] to uncover the morphology of individual neurons. To determine the identity of the neurons labelled, we leveraged the connectome of the adult fly brain as a reference and compared the morphology of the neurons identified by light microscopy with the ones in the connectome dataset using the FlyWire database[30,42] (codex.FlyWire.ai; see Methods). Five out of six Notch^{On} clusters corresponded to different projection neurons in FlyWire, all of them terminating in deep layers of the lobula (Lo5-Lo6): TmY11 (c45), TmY10 (c52), Tm8a (c53), Li06/Tm24 (c69), and Tm5f (c82) (**Supp. Fig. 3B-F, B'-F'**), in agreement with our previous results for the known main OPC neurons (see **Fig. 1E**). Moreover, we used the neurotransmitter predictions of these "morphological types" from FlyWire[30,42,51] (score ranging from 99 to 100% prediction accuracy) to confirm that these neurons were cholinergic[11] (**Supp. Fig. 3B'-F')**. The heterogeneous (containing more than one cell type, see Methods) cluster 59,

labelled a neuron with glutamatergic identity and unlikely to be of main OPC origin (see **Supp. Fig. 4G**).

In the case of Notch^{Off} neurons from the same late temporal window, the split-Gal4 line for c38 labelled an interneuron targeting medulla layers M6 and M7 that morphologically matched Sm03 neurons in FlyWire and had glutamatergic identity (90% prediction accuracy)[30,42] (**Supp. Fig. 3G-G'**). **Suppl. Fig. 4H** describes the non-main OPC neurons labelled by the heterogeneous cluster c39. Furthermore, we determined the expression of specific TFs in both Notch^{On} and Notch^{Off} clusters to validate their assignment to these specific neuronal morphologies (**Supp. Fig. 3B-G**, **Supp. Fig 4I-N**).

Together, these results indicate that the newly annotated late born Notch^{On} neurons from the sixth (Hbn/Opa/Slp) temporal window are projection neurons that terminate at deep layers of the lobula neuropil, as was the case for the neurons previously known from this temporal window (**Fig. 1E**), whereas Notch^{Off} neurons are interneurons targeting the distal medulla (previously known interneurons from this window) (**Fig. 1D**) or the serpentine layer.

Using the same strategy, we identified that Sm01 and Sm02, which target the serpentine layer (M7), were generated from the last D/BarH1 temporal window (corresponding to the Notch^{Off} cluster 129, which is heterogeneous) (**Supp. Fig. 5A-D'**). Known Notch^{Off} neurons form this temporal window are Dm2, Mi15 (which should be re-named Sm44 following the nomenclature from FlyWire, see Methods) and T1. Together with the above analysis using previously annotated neurons, these results indicate that Distal medulla and at least 3 Sm neurons are all born from late temporal windows.

All the main OPC Notch^{On} projection neurons currently identified terminate at deep lobula layers (Lo5-Lo6) if they are born after the fifth temporal window. However, Notch^{Off} projection neurons born in earlier windows 3rd (Opa/Erm: Tm5c) or 4th (Erm/Ey: Tm5d and TmY5a), target deep lobula layers (Lo5-Lo6) (**Fig. 1E**). To determine whether the three unannotated neurons from the 4th Erm/Ey temporal window (**Supp. Fig 6A**) also target deep lobula layers, we generated split-Gal4 lines for clusters 26, 41, and 54, and identified Tm33, Tm5e, and potentially Sm14, to correspond to these clusters, respectively (**Supp. Fig 6B-E'**). Both Tm33 and Tm5e target deep lobula layers (Lo5 and Lo6, respectively), while Sm14 targets M7. Hence, these results indicate that all the Notch^{Off} projection neurons born in the 4th Erm/Ey temporal window target deep layers of the lobula neuropil (Lo5-Lo6).

In summary, we annotated 10 additional neurons from late (Hbn/Opa/Slp and D/BarH1) and early (Erm/Ey) temporal windows, which have the same termination pattern as the previously annotated neurons from these windows (**Fig. 1E**).

We next determined the neuropil synapse location of these newly annotated main OPC neurons. As shown in **Figure 4,** the newly annotated Notch^{On} and Notch^{Off} neurons share similar neuropil pre- and postsynapse location with the previously known main OPC neurons from the same temporal window and Notch status. Both presynapses and postsynapses of Notch^{Off} interneurons Sm01 and Sm02 from the D/BarH1 window were in the Distal medulla (**Fig. 4A-A'**), in the same manner as the previously known neurons from this temporal window (**Fig. 3A-A'**). Sm03 synapses were located in similar layers (**Fig. 4B-B').** Moreover, both presynapses and postsynapses of Erm/Ey Notch^{Off} projection neurons (Tm33, Tm5e) were in the M6-M7 layers (**Fig. 4A-A'**) and deep layers of the lobula (**Fig. 4D-D'**), in the same manner as the previously known main OPC neurons from this window (**Fig. 3A-A', D-D'**).

The newly annotated Notch^{On} (Tm8a, Tm5f, Li06/Tm24, TmY10 and TmY11,) and Notch^{Off} (Sm03) neurons from the Hbn/Opa/Slp temporal window contained most of their presynapses and postsynapses in the Distal medulla (**Fig. 4B-B'**), in the same manner as the previously known main OPC neurons (**Fig. 3B-B'**). Moreover, newly annotated Notch^{On} projection neurons from this temporal window made most of their synapses in the deepest layers of the lobula (**Fig. 4C-C'**), in the same manner as the previously known main OPC projection neurons from this temporal window (**Fig. 3C-C'**).

In summary, these results indicate that the temporal cascade in main OPC NBs, together with Notch identity, generate neurons with similar targeting, both for pre- and postsynapses.

Temporal origin of unannotated main OPC neurons can be inferred from neuropil synapse location

Next, we wanted to determine whether neuropil synapse location could serve to inform temporal origin of unannotated (48 out of 103) main OPC neurons (**Fig. 1C**). Optic lobe neurons are generated from different progenitor regions: main OPC, tOPC, IPC, and Central Brain[7-9,11-12,28,52-54]. The neuronal progeny from each of these regions occupy specific locations within the optic lobe in the adult, which serve as a proxy of their developmental origin[28,55]. For example, main OPC neurons have their somas in the medulla cortex in the adult brain. Hence, we selected neurons with somas in the medulla cortex in the FlyWire dataset as a proxy of the putative (unannotated) main OPC neurons (see **Supp. Fig. 7A** for a tree of all known and putative main OPC neurons representing their connectivity similarity) and plotted their synapse location using their EM coordinates from FlyWire[30,42].

We compared synapse location of unannotated main OPC neurons with that of annotated neurons for which we knew their temporal origin (**Fig. 5; Supp. Tables 2-3**). Neurotransmitter identity of unannotated main OPC neurons in FlyWire provides additional information about the putative Notch identity of these neurons (**Supp. Fig. 1C**), which can in turn inform temporal origin. For example, all main OPC cholinergic neurons are Notch^{On}, while all main OPC GABAergic neurons are Notch^{Off} and most glutamatergic neurons are Notch^{Off} (except a few that are Notch^{On} and correspond to the D/BarH1 temporal window)[11]. Hence, as can be inferred by the pre- and postsynapses location in deep layers of the lobula of unannotated main OPC cholinergic (Notch^{On}) projection neurons such as Tm7, Tm8b, Tm16, Tm36, Tm37, TmY9q, TmY9q⊥, TmY20 and TmY31 (**Fig. 5A-B**), it is likely that these are mostly generated from the Hbn/Opa/Slp and/or the Slp/D temporal windows (**Fig. 5A"-B"**). Since we do not have split-Gal4 lines to label additional unannotated neurons from these windows, we used a driver line (R80G09(*ham*)-Gal4) to label late born Toy+ neurons, which are generated from the Hbn/Opa/Slp and the Slp/D temporal windows[11]. This driver line labelled projection neurons targeting deep layers of the lobula throughout development (**Supp. Fig 8A-D**), and MCFO[36] using this driver line in the adult labelled projection neurons targeting deep layers of the lobula, that we could identify as Tm5f (c82) and Tm36 (**Supp. Fig. 8E-G**). Based on specific TF expression Tm36 likely corresponds to cluster 59 of the Hbn/Opa/Slp temporal window (**Supp. Fig. 8E-I**). Moreover, cell number for each specific morphological type in the adult EM dataset[30,42] can be leveraged to inform the putative scRNA-seq clusters these morphological types correspond to (see Methods).

In the case of unannotated GABAergic Notch^{Off} neurons LMa2, LMa3, and LMa4, which mainly target the superficial lobula, the number of possible temporal origins ranges from the Hth to the Hbn/Opa/Slp windows (**Fig. 5A-A'-B-B'**). However, since GABAergic neurons only

originate from the Hth, Hth/Opa, and Ey/Hbn/Opa temporal windows (**Fig. 1C**) (Konstantinides et al., 2022), this reduces to three the possible temporal origins for these neurons.

For the medulla neuropil, since synapses from different temporal origins are not as nicely segregated as in the lobula, it is more difficult to infer temporal origin from synapse location (**Supp. Fig. 9A-B**). However, all the Pm neurons are GABAergic ($Notch^{Off}$), and hence they are born from either the Hth, Hth/Opa, or Ey/Hbn/Opa temporal windows[11] (**Fig. 1C**). However, based on synapse location of known main OPC Pm neurons it is more likely that the six remaining unannotated Pms are born from either the Hth or the Hth/Opa temporal windows (**Supp. Fig. 9B-B'**).

In summary, our data indicate that it is possible to infer the temporal origin of unannotated main OPC neurons from connectomic data leveraging patterns of targeting of known main OPC neurons. In the future, the availability of additional cluster-specific split-Gal4 lines will allow to test more correlations between targeting and temporal window of origin.

Neuropil targeting of main OPC neurons is associated with specific visual functions

Specific neuropil layers in the optic lobe are associated with specific visual functions. For example, medulla M3 and M6, the recipient layers of the color photoreceptors R8 and R7, respectively, are mainly involved in processing color information[56-58]. Since main OPC neurons with specific temporal and Notch identities target their synapses to specific layers, we next asked whether shared synapse location of main OPC neurons is associated with specific visual functions.

The function of only a small percentage of main OPC neurons has been experimentally tested[59-61]. The adult fly brain connectome has recently developed a prediction of the putative functional modalities of each (intrinsic) optic lobe neuron, which defined "connectomic" cell types based on shared connectivity vectors and then grouped these different connectomic types in specific functional classes based on the nature of their main inputs and outputs, as well as previous experimental knowledge about the function of specific neurons in each group[30]. The authors defined nine different functional subsystems: Motion, ON, OFF, Object, Form, Luminance, Color, Polarization, and Photoreceptors. ON and OFF components receive strong inputs from R1-R6 photoreceptors and contain neurons previously described to comprise the ON and OFF motion detection pathways[30]. Hence, we merged Motion, ON, and OFF into the "Motion circuits" modality and kept the other groups as individual modalities.

We first looked at the location of pre- and postsynapses of all annotated main OPC neurons and color-coded them based on their predicted functional identity. As shown in **Figure 6,** synapses of previously annotated neurons (circles) and synapses of neurons annotated in this work (triangles) have a similar distribution, both in the medulla and lobula neuropils that is linked to their predicted visual function (see below). Interestingly, all the newly annotated neurons are predicted to be involved in Color vision, in agreement with their targeting to Distal medulla layers, which are the recipient of color photoreceptors R7 and R8, and deep lobula layers (see below).

In the medulla neuropil, both pre- and postsynapses of $Notch^{Off}$ neurons that contribute to the Object subsystem are enriched in the Proximal medulla, while synapses of $Notch^{On}$ neurons that contribute to this modality are enriched in the Distal medulla (**Fig. 6A-A'-B-B'**). Interestingly, all the pre-and postsynapses of neurons ($Notch^{On}$ and $Notch^{Off}$) contributing Form circuits are enriched in the Distal medulla (**Fig. 6A-A'-B-B'**). Moreover, $Notch^{Off}$ neurons contribute all the synapses of the Luminance modality, which are enriched in the Distal medulla (**Fig. 6A-A'**). Pre- and postsynapses of neurons involved in Polarization (DmDRAs, $Notch^{Off}$ identity) are enriched in the M6-M7 layers, and they are restricted to the dorsal part of the medulla, which receives input

from the Dorsal Rim area of the retina that detects skylight polarization[62] (**Fig. 6A-A'**). Postsynapses of Notch^{On} neurons, as well as pre- and postsynapses of Notch^{Off} neurons from Motion circuits are enriched in the Distal medulla, where they receive inputs from lamina (L1-L5) neurons (**Fig. 6A-A'-B-B'**). However, presynapses of Notch^{On} neurons from Motion circuits are enriched in the Proximal medulla, where they provide inputs to T4 neurons. In the case of Color neurons, their pre- and postsynapses are enriched in the Distal medulla, independently of their Notch status, in agreement with the location of color photoreceptors (R7/R8) in this region of the medulla (**Fig. 6A-A'-B-B'**).

In the lobula, neurons from Motion circuits are enriched in superficial layers, while neurons from Form and Color subsystems mostly target deeper layers (**Fig. 6C-C'-D-D'**). Hence, Form and Color circuits are segregated from Motion in the lobula neuropil. In contrast, Object circuits are distributed all over the lobula (**Fig. 6C-C'-D-D'**).

Finally, there was no significant association between synapse location and functional modalities of annotated main OPC neurons in the lobula plate neuropil (**Supp. Fig. 10; Supp. Table 1**). Since compared to the medulla and lobula neuropils, there are fewer neurons targeting the lobula plate that are annotated, the predictive power is low.

Hence, these results show that main OPC neurons involved in the same functional modalities target their synapses to similar regions of the medulla and lobula neuropils.

Next, we wanted to determine how generalizable was the link between neuropil synapse location and specific functional modalities by analyzing the synapse location of putative main OPC neurons using their EM coordinates from FlyWire[30,42]. Notably, putative main OPC neurons with the same predicted function as previously annotated main OPC neurons share synapse location pattern in both the medulla and lobula neuropils (**Supp. Fig. 11**).

- In the medulla, both pre- and postsynapses of putative main OPC neurons from Polarization and Form circuits localize to similar regions as the previously known main OPC neurons, i.e. mainly to the Distal medulla and the Serpentine layer (**Supp. Fig. 11A-A"-B-B")**. Pre- and postsynapses of putative main OPC neurons from Object and Color circuits share a similar pattern to that of known main OPC neurons, with Object synapses enriched in the Proximal medulla and Color synapses in the Distal medulla, although these synapses are more restricted to the middle layers of the medulla (**Supp. Fig. 11A-A"-B-B")**, in agreement with the majority (33 out of 50) of putative main OPC neurons involved in Color vision being Sm neurons (**Supp. Fig. 7**).

In the lobula, pre- and postsynapses of both annotated and putative main OPC neurons involved in Form and Color vision are enriched in deep layers of the neuropil (**Supp. Fig. 11C-C'-D-D'**). Moreover, the presynapses of putative main OPC neurons of the Object subsystem share a similar neuropil distribution in intermediate lobula layers with the known Notch^{On}, but not with the known Notch^{Off} neurons (**Supp. Fig. 11C-C'**). The postsynapses of both annotated and putative main OPC neurons from the Object subsystem are enriched in superficial layers of the lobula (**Supp. Fig. 11B-B'**). Interestingly, the pre- and postsynapses of TmY20, the only unannotated main OPC neuron from Motion circuits with synapses in the lobula, follow the opposite pattern to the ones from previously annotated main OPC neurons, with synapses located in deep lobula layers instead of in the superficial ones (**Supp. Fig. 11C-C'-D-D'**). Notably, although TmY20 receives inputs from motion-sensitive T4 and T5 neurons in the lobula plate[63], it groups with main OPC neurons involved in Color or Form vision based on connectivity, in agreement with their synapses being located in deep layers of the lobula neuropil (**Supp. Fig. 7**).

Finally, in the lobula plate, only presynapses of putative main OPC neurons from the Color subsystem share a similar pattern (in Lop2-Lop3) to the presynapses of known main OPC neurons (**Supp. Fig. 12A-A'-B-B'**). Moreover, different visual modalities are not associated with specific lobula plate layers (**Supp. Fig. 12A-A'-B-B'**).

Altogether, these results indicate that main OPC neurons with similar functions target their synapses to similar medulla and lobula layers.

Link between temporal origin and visual function of main OPC neurons

Finally, we asked whether specific temporal windows contributed neurons from specific functional subsystems. Specific temporal origins were significantly associated with Object (Hth), Form (Slp/D), and Color (Hbn/Opa/Slp), but not with Motion, Luminance, or Polarization subsystems (**Supp. Fig. 13A-F; Supp. Table 3)**. Adding Notch identity to temporal origin, the Object subsystem was significantly associated with Hth+Notch^{Off} identity, Form with Slp/D+Notch^{Off} identity, and Color with Hbn/Opa/Slp+Notch^{On} identity (**Supp. Fig. 13A-F; Supp. Table 3)**. However, there was no significant association between Notch status alone and either of the functional modalities (**Supp. Fig. 13 G-L; Supp. Table 3**), which was expected, since Notch identity mainly determines projection neuron vs interneuron fate.

Moreover, none of the temporal windows produced neurons from all the functional subsystems, with specific temporal windows producing neurons ranging from 2 (i.e., Hth and Opa/Erm, producing neurons from both Object and Motion circuits, and both Color and Luminance, respectively) to 5 (i.e., Hbn/Opa/Slp) subsystems (**Supp. Fig. 13M**). Interestingly, Form circuits were all comprised of neurons generated from a single temporal window (Slp/D). The three Dm3 types (p, q, v) recently identified in the adult brain connectome[30,42-43], together with TmY4, TmY9q, and TmY9q⊥ neurons were hypothesized to constitute a circuit for Form vision[64]. From our data, at least two Dm3 subtypes (p and q) and TmY4 are born in the same late temporal window (Slp/D)[11] (**Fig. 1C**). Notably, since all the synapses from Form circuits localize to similar Distal medulla and deep lobula layers **(Supp. Fig. 11**), it is likely that the unannotated neurons from the Form subsystem, Dm3v, TmY9q, and TmY9q⊥ (see **Fig. 5** and **Supp. Fig. 9**), are also late born, likely within the same Slp/D temporal window as the annotated Form circuit neurons (**Supp. Fig. 13M**).

Discussion

Neuronal specification mechanisms set the wiring plan of the adult brain

We sought to understand the link between the specification of main OPC neurons and their morphological (targeting and synapse location) and functional features. As we have shown here, both temporal patterning and Notch identity determine specific characteristics of main OPC neurons (projection neuron *vs.* local interneuron, targeting depth, synapse location, neurotransmitter identity, etc) that are progressively set up during development.

We have shown an association between main OPC Notch^{On} projection neurons temporal identity and lobula layer targeting depth in the adult brain, which is established early in development and genetically determined (**Figs. 1-2**). However, early born Notch^{Off} neurons from the Opa/Erm (3rd) and Erm/Ey (4th) windows target deep layers of the lobula, suggesting that they might have a different regulation of axon targeting. Notably, it has been recently proposed that Notch signaling in Notch^{On} projection neurons activates Netrin expression and inhibits the

repulsive receptor unc-5, a process necessary for correct lobula layer targeting[65]. Moreover, most of the Notch^{Off} neurons express Unc-5, except a stripe of Notch^{Off} neurons likely born around the Ey temporal stage and that could correspond to Knot+ neurons, which turn off unc-5 regardless of their Notch status[65]. Hence, these Notch^{Off} neurons could correspond to the early born Knot+ projection neurons that target deep layers of the lobula, which target the lobula through a different mechanism than Notch^{On} projection neurons. Moreover, Notch^{Off} neurons (up to the D/BarH1 temporal window) are either glutamatergic or GABAergic[11], and hence likely inhibitory, which could explain why these neurons behave differently than cholinergic Notch^{On} excitatory neurons. Hemilineage-specific targeting has also been shown in the fly VNC, where interneurons from Notch^{On} hemilineages project to the dorsal motor neuropil, whereas Notch^{Off} hemilineages project to the ventral sensory neuropil, indicating that neurons from different hemilineages respond differently to pathfinding cues[21].

Furthermore, by leveraging the complete EM reconstruction of the adult fly brain[30,42], we have shown that the temporal origin and Notch status of main OPC neurons is significantly associated with their synapse distribution in the adult brain (**Fig. 3**). Importantly, our results show that lineage relationship (temporal and Notch identity) can predict main OPC synapse location in the adult optic lobe (**Fig. 4; Supp. Figs. 3-6**), indicating that the temporal cascade in main OPC NBs and Notch signaling in GMCs generate neurons with similar targeting and hence connectivity.

As mentioned above, we have shown that neuropil targeting depth of main OPC projection neurons is established early in development (**Fig. 2**). In the same manner, we recently showed that main OPC neurons neurotransmitter identity is established as soon as they are born, as they express transcripts of neurotransmitter-related genes already at larval stages[11]. This indicates that genetic programs in main OPC neurons determine their morphological and functional identities already at neurogenesis stages, which are subsequently refined during later targeting stages and synaptogenesis. In this sense, we have recently shown that on average 10 different terminal selector TFs are expressed in each optic lobe neuronal type, whose expression is maintained from neurogenesis stages to adult[66-67]. Notably, most of the genes that we used to identify neurons born at different times in the temporal cascade by their concentric pattern of expression in the medulla cortex[11,44], were predicted to act as terminal selectors throughout development[25,67] (**Supp. Fig. 14A**). Moreover, we have recently shown that these genes carry the same information about neuronal identity as the sum of the temporal+spatial+Notch origins information encoded in progenitors[25], highlighting the importance of these selector genes to establish specific neuronal identities and its maintenance. In the future, it will be important to understand how they control the expression of specific Cell Surface Molecules and functional genes in specific neuronal types, for example, the expression of the histamine receptor Ort, which is expressed in neurons involved in color vision[68], and which is expressed in main OPC neurons targeting the Distal medulla and deep lobula layers in the adult (**Supp. Fig. 14B**).

The link between temporal identity and specific projection patterns has been previously shown in different systems, although without cell-type specificity in most cases. Projection neurons in the fly olfactory system create a protomap of dendritic targeting that is correlated with birth order and lineage identity[69]. In the mammalian cortex, the relationship between temporal identity and the projection pattern of excitatory cortical neurons has long been known, with early born layer VI corticothalamic and layer V subcerebral projection neurons projecting to the thalamus and subcortical structures (e.g. spinal cord and superior colliculus), respectively, and later born upper layer neurons projecting within the cortex, such as locally projecting stellate neurons in layer IV and contralateral callosal projection neurons in layer II/III[70-73]. In the mammalian spinal cord, birth

order has been linked to projection range: Early-born neurons project long-range, while later-born neurons project locally within the spinal cord[74]. Hence, the ordered and stereotyped generation of neurons with different projection patterns underlines how temporal patterning contributes to the ordered generation of neuronal circuits.

Predicting targeting and connectivity from developmental origin and vice versa

The fly devotes more than half of its brain to visual processing. Although extensive functional work has allowed a mechanistic understanding of motion vision and, to a lesser extent, color vision in the fly[56-61], the developmental origin of different circuit components has been less studied[52-54,75]. By leveraging predicted functional data from connectivity[30], we have linked the temporal origin and synapse location of main OPC neurons to their main visual modality: Motion, Object, Form, Luminance, Polarization, and Color vision. We have shown that main OPC neurons with similar temporal origin and Notch identity target similar neuropil layers and are involved in similar visual functions (**Figs. 3-6**). Importantly, we extended these observations to all the putative main OPC neurons, by analyzing the synapse location and predicted functional modality of all the optic lobe neurons with somas in the medulla cortex (**Fig. 5; Supp. Figs. 9, 11**).

Furthermore, synaptic coordinates in both the medulla and lobula neuropils of putative main OPC neurons and Notch status inferred from neurotransmitter identity[30,42,51], allowed us to predict their approximate temporal identity, which was validated in the case of Tm36 projection neurons (**Supp. Fig. 8**). In the future, it would be important to test other predictions by annotating additional clusters. We did not find, however, a clear association between temporal origin and synapse location in the lobula plate neuropil. Developmentally, this neuropil mainly depends on the specification of the four subtypes of T4 and T5 IPC neurons that are all born at the same time[52-53,75], which might explain why synapse location of main OPC neurons in this neuropil is not associated with their temporal origins. Notably, the medulla neuropil, whose neurons are generated mostly from the main OPC, is the optic lobe region with the most input and output connections[30,42-43], highlighting the importance of this study to understand the link between optic lobe development and connectivity.

Linking the optic lobe transcriptome to the connectome

To obtain a comprehensive view of the neuronal diversity of the brain, it is essential to match transcriptomic types to morphological ones. We and others have previously identified around 172 distinct neuronal and 19 glial clusters in the adult brain[31-33]. Recently, the complete EM reconstruction of the adult fly brain identified 227 distinct morphological and connectivity neuronal types intrinsic to the optic lobe, and around 500 that connect the optic lobe with the central brain (called boundary types)[30,42], indicating an underestimation of transcriptomic types in our dataset[33]. In fact, the integration of our optic lobe dataset with the one from Kurmangaliyev et al.,[32] indicates that some of our clusters (31 out of 172) are indeed heterogeneous and contain more than one cell type[25]. Furthermore, most of the neurons whose somas are at the border between the optic lobe and the central brain might not have been dissected out in our single-cell preparation of isolated optic lobes. This work provides annotations for 9 additional main OPC neuronal clusters (**Supp. Fig. 3-6**). Notably, by building additional split-Gal4 lines designed based on the co-expression of gene pairs in each neuronal cluster[46,50], the identification of most of the optic lobe neuronal morphologies and their assignment to both specific transcriptomic clusters and EM types is within reach. It is important to note however that splitting heterogeneous clusters in our scRNA-seq dataset into individual neuronal types, which can be achieved by leveraging multiome datasets,

will be necessary to annotate most of them, since the use of split-Gal4 lines to identify neuronal morphologies in some heterogeneous clusters was not an efficient way to identify specific neuronal identities (e.g, c39 and c59, **Supp. Fig. 4**).

The completion of the adult fly brain connectome has identified new neuronal classes and subtypes[30,42]. For example, although only 3 different subtypes of Tm5 neurons, Tm5a, Tm5b, Tm5c, were previously described[34,76], the EM reconstruction identified 3 more subtypes: Tm5d, Tm5e, and Tm5f[30]. Our approach using specific split-Gal4 lines together with sparse labelling allowed us to identify the potential clusters corresponding to these 3 types: Tm5d (c55, previously named as Tm29), Tm5e (c26), and Tm5f (c82), providing genetic access to these neurons for functional studies aiming at investigating them. Like Tm5a-b-c, types, Tm5d-e-f are part of the Color functional modality[30] (**Supp. Fig. 7**). Furthermore, we identified the clusters for two types of Sm neurons, Sm01 and Sm02, that are biased for a yellow or pale column, since Dm8b (corresponding to pDm8 in Nern et *al.*,[43] and potentially in Matsliah et *al.*,[30]) contributes 33.5% of the synapses to Sm01, while Dm8a (yDm8) contributes 10% of the synapses (**Supp. Fig. 15**). In the same manner, the main synaptic partner of Sm02 is Dm8a (51.6% synapses) vs 7.3% input from Dm8b, indicating again that Sm02 is biased to a pale vs yellow column. These, together with Tm5a and p/yDm8 neurons[34,76-79]provide additional examples of R7/R8 column selectivity and agrees with the placement of Sm01 and Sm02 as part of the color vision circuit subsystem[30].

In conclusion, this work links both the temporal and Notch origins of an entire progenitor region, the most diverse in the fly optic lobe, to their synaptic targeting, connectivity and their putative function in the adult brain.

Acknowledgements

We thank the Desplan lab, especially Ryan Loker, for critical reading of the manuscript. We thank Bloomington *Drosophila* Stock Center for stocks (NIH P40OD018537). We also thank the FlyLight team at Janelia for providing the R13E12-LexAp65 plasmid and Yuh-Nung Jan for providing the anti-Ham antibody. The Desplan laboratory was supported by grants from the National Eye Institute R01EY017916 and R01EY13010. I.H. was supported by a Human Frontier Science Program Postdoctoral Fellowship LT000757/2017-L, by a senior postdoctoral fellowship from the Kimmel Center for Stem Cell Biology and by a Marie Sklodowska-Curie Postdoctoral Fellowship (101154260). Y.-C.C. was supported by New York University (MacCracken Fellowship), by a NYSTEM institutional training grant (Contract #C322560GG), and by a Scholarship to Study Abroad from the Ministry of Education, Taiwan. Y.-C.D.C. was supported by the NIH National Eye Institute (F32EY032750 and K99EY035757). F.S. was supported by New York University (MacCracken Fellowship and Dean's Dissertation Ph.D. Fellowship). A.G.G was supported by a DURF fellowship from NYU. J.D.R was supported by the NYU Simon's Foundation SURP fellowship. S.C. was supported by an EMBO Long-Term Postdoctoral Fellowship (ALTF 319-2019).

Author contributions

I.H. and C.D. conceived the project and wrote the manuscript. I.H. designed all the experiments. I.H., A-G.G., Y.-C.D.C., J.D.R and S.C.C performed the experiments. Y.-C.C performed the connectivity analyses from FlyWire. I.H., Y.-C.C., and F.S. analyzed the data. Y.-C.D.C. built the split-Gal4 lines. F.S. wrote the code for the generation of the heatmaps.

Declaration of Interests

The authors declare no competing interests.

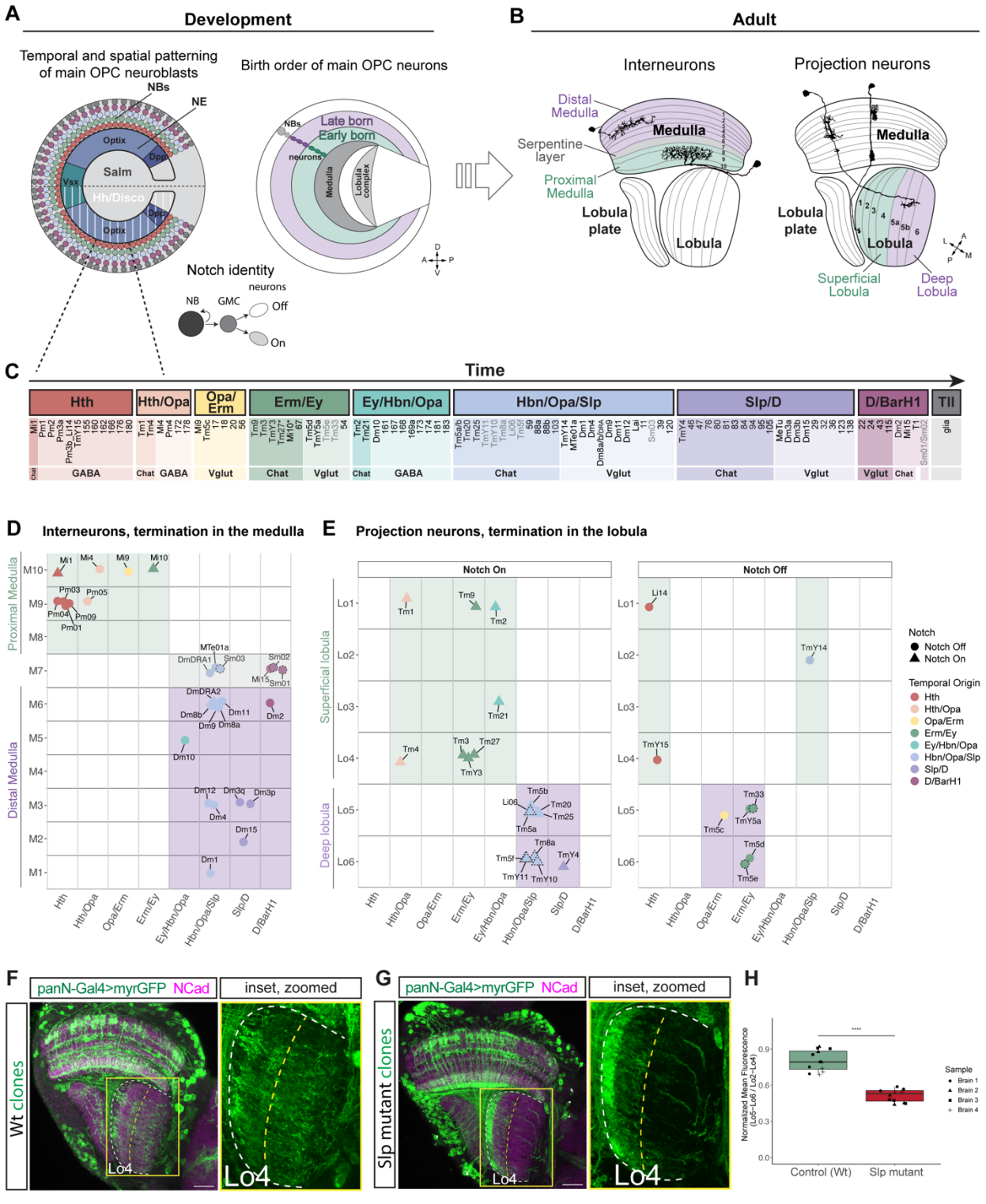

Figure 1. Link between temporal identity and neuropil targeting depth of main OPC neurons.
A. Spatial and temporal patterning of main OPC progenitors and Notch signaling specify medulla neural diversity. Left. Lateral view of the main OPC neuroepithelium (NE) at L3 stage, showing the domains of expression of the spatial factors Optix, Dpp, and Vsx. Salm is expressed in the dorsal half of the main OPC, while Hh and Disco are expressed in the ventral half (white vertical lines). All the neuroblasts (NBs, represented as spheres) generated from each main OPC spatial domain undergo the same cascade of temporal TF expression (represented as different colors). Notch signaling in intermediate progenitors (GMCs) specifies two different neurons, Notch^{On} and Notch^{Off}. **Right.** Lateral view of the main OPC neuronal layer at L3 stage, showing the columnar arrangement of main OPC neuronal somas, with early born neurons (green ovals) located closer to the developing medulla neuropil (dark gray crescent) and later born neurons (purple ovals) located farther. A: anterior, P: posterior, D: dorsal, V: ventral.
B. Neuronal classes of the main OPC in the adult brain. Cross-section of the adult optic lobe, with the medulla, lobula, and lobula plate neuropils represented. One Pm interneuron, one Dm interneuron, and two Transmedullary projection neurons are represented. The different layers of the medulla and the lobula neuropils are numbered. A: anterior, P: posterior, M: medial, L: lateral. **C**. **Temporal patterning generates main OPC neurons in a stereotyped order.** Broad temporal windows of origin of main OPC neurons, from Konstantinides *et al.*, 2022[11]. Different temporal windows generate different number of neurons, since spatial patterning does not affect all the NBs output in the same manner. The specific neuronal types and clusters generated in each temporal window are indicated, from Konstantinides *et al.*, 2022[11]. Clusters in grey indicate the ones annotated in this work. Transient Extrinsic (TE) neurons (Notch^{On} clusters 220, 223, 224 and 233, from the Hth temporal window) are not included, since they die before adulthood and hence, they are not present in the adult connectome. Within each temporal window, Notch^{On} neurons are shown in darker colors than Notch^{Off} neurons. Neurotransmitter identity is indicated. Neurons with an asterisk indicate unannotated neurons born in the Erm/Ey temporal window.
D. Relationship between temporal origin of main OPC interneurons and layer targeting depth. Plot representing known main OPC interneurons from each temporal window and the medulla layer each neuron terminates in the adult brain. Proximal medulla is shown in green, the Serpentine layer in grey, and Distal medulla in purple. Neurons annotated in this work are indicated with a black dashed line.
E. Relationship between temporal origin of main OPC projection neurons and lobula layer targeting depth. Plot representing known main OPC projection neurons from each temporal window and the lobula layer each neuron terminates in the adult brain. Superficial lobula (Lo1-Lo4) is shown in green and deep lobula (Lo5-Lo6) in purple. Temporal origin is color-coded. Notch^{On} neurons are represented as triangles, while Notch^{Off} neurons are represented as circles. Neurons annotated in this work are indicated with a black dashed line. Other projection neurons such as T1 (targeting both the Distal medulla and lamina) and MTe01a and MeTu (targeting both medulla and central brain) are not indicated.
F. Stopping the temporal cascade at late temporal windows reduces the neuronal projections in deeper layers of the lobula neuropil. (**F**) Wild-type NB MARCM clones labelled using the pan-neuronal driver nSyb(R57C10)-Gal4. Inset: zoomed image of the lobula neuropil. (**G**) Slp mutant NB MARCM clones labelled using the pan-neuronal driver nSyb(R57C10)-Gal4. Inset: zoomed image of the lobula neuropil. The outline of the lobula is indicated with a white dashed line, while Lo4 layer is indicated with a yellow dashed line. Scale bars: 20 µm. (**H**) Ratio of normalized mean fluorescence between Lo5-Lo6 and Lo2-Lo4 layers in control (Wt) and Slp mutant brains. ****p = 6.12E-06 (two-way ANOVA).

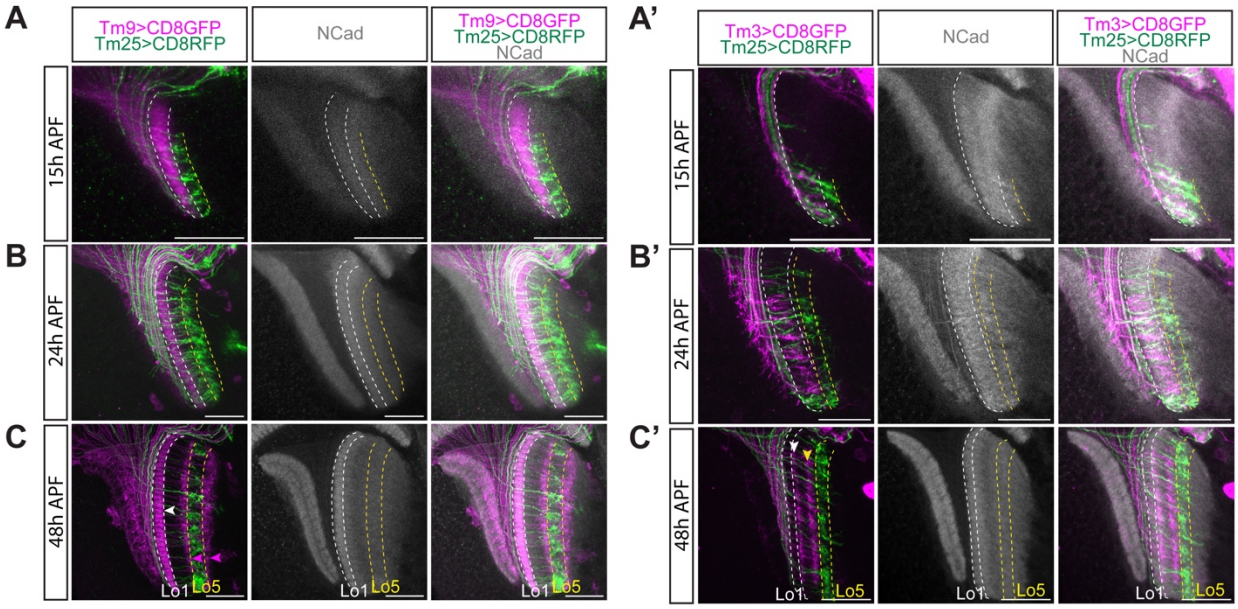

Figure 2. Lobula layer targeting of main OPC projection neurons is established early.
A-C'. Protolayer targeting of either Tm9 or Tm3 (magenta) and Tm25 (green) Notch^{On} projection neurons at 15 (**A-A'**), 24 (**B-B'**) and 48 (**C-C'**) hours after puparium formation (APF). At 48h APF the Tm9 driver line labels additional neurons targeting Lo4 and Lo6 (magenta arrowheads in C). NCad indicates the developing lobula (with protolayers indicated in white for Tm9 and Tm3 and in yellow for Tm25) and lobula plate neuropils at different stages. At 48h APF Lo1 is indicated in both C and C' and the arbors of Tm3 in Lo2 and Lo4 are indicated with a white and yellow arrowheads, respectively. Scale bars: 20 µm.

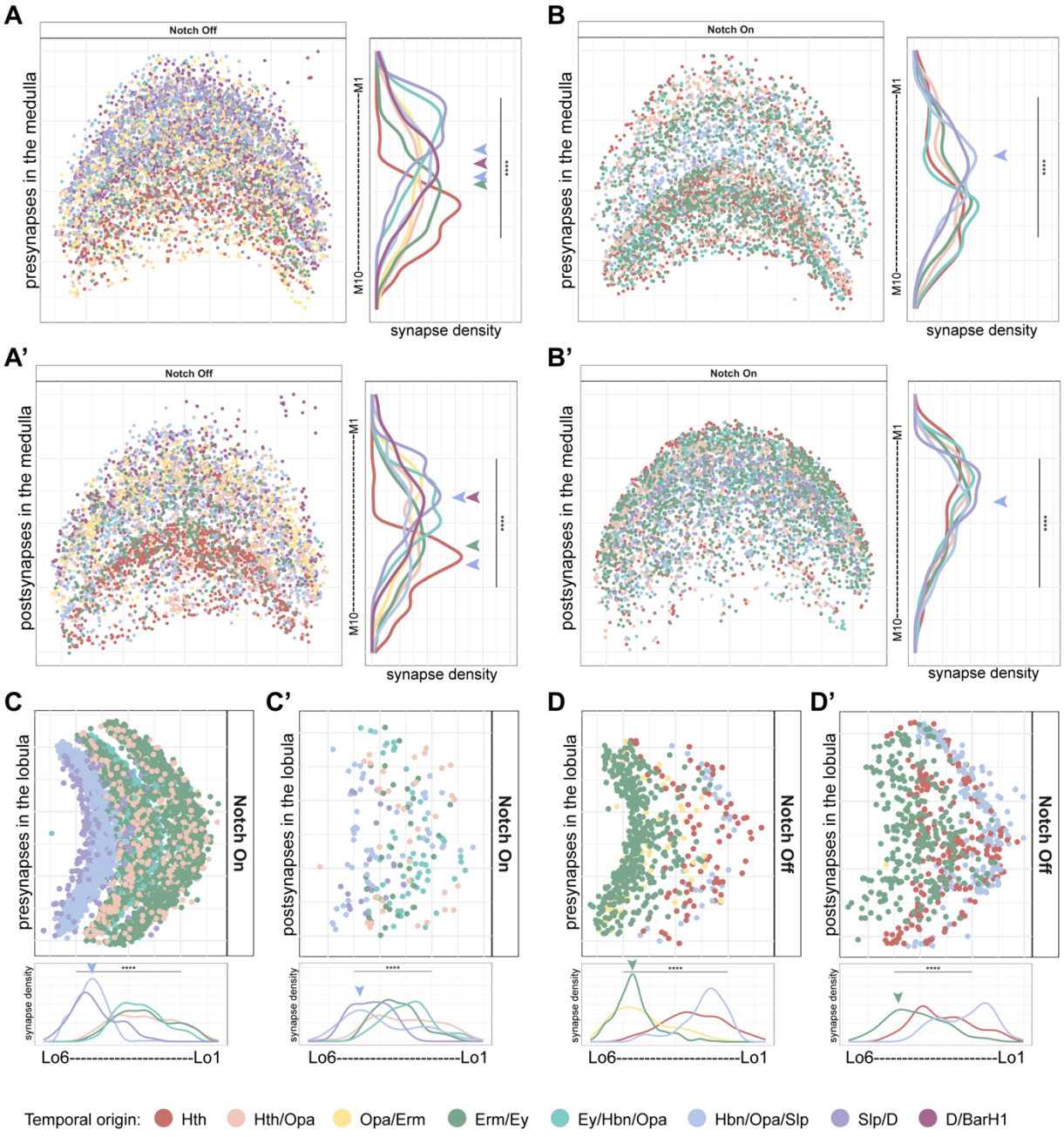

Figure 3. Neuropil synapse location is associated with specific temporal origins.
Pre- (**A-B**) and postsynapse (**A'-B'**) distribution in the medulla neuropil of annotated Notch^{Off} (**A-A'**) and Notch^{On} (**B-B'**) main OPC neurons. Pre- (**C-D**) and postsynapse (**C'-D'**) distribution in the lobula neuropil of annotated Notch^{On} (**C-C'**) and Notch^{Off} (**D-D'**) main OPC neurons. Synapses are color-coded based on temporal window of origin, from Konstantinides *et al.*, 2022[11]. Curve graphs indicate synapse density along the neuropil, color-coded by temporal window of origin. Arrowheads indicate peaks of synapse density of main OPC neurons from the indicated temporal windows.
Statistical comparisons of synaptic depths between different temporal origins and Notch states were performed using Kruskal-Wallis tests followed by Dunn's post-hoc tests (FSA package), with P-values adjusted using the Bonferroni method (see Supp. Table 1 for one-to-one comparisons between temporal windows).

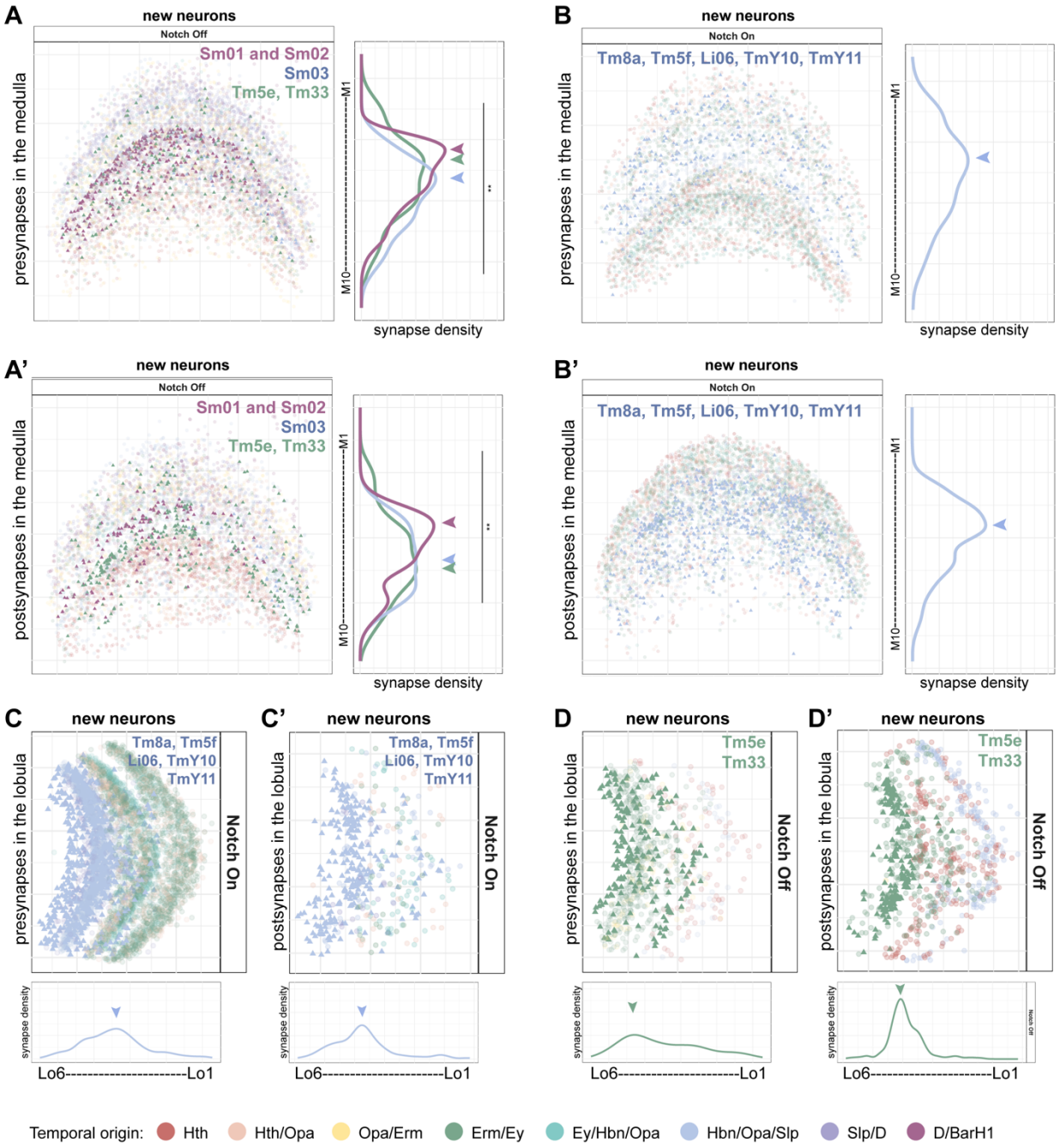

Figure 4. Temporal identity of main OPC neurons predicts their neuropil synapse location in the medulla and lobula neuropils. Pre- (**A-B**) and postsynapse (**A'-B'**) distribution in the medulla neuropil of Notch^{Off} (**A-A'**) and Notch^{On} (**B-B'**) main OPC neurons annotated in this work. Pre- (**C-D**) and postsynapse (**C'-D'**) distribution in the lobula neuropil of Notch^{On} (**C-C'**) and Notch^{Off} (**D-D'**) main OPC neurons annotated in this work. Synapses are color-coded based on temporal window of origin, from Konstantinides *et al.*, 2022[11]. Curve graphs indicate synapse density along the neuropil, color-coded by temporal window of origin. Arrowheads indicate peaks of synapse density of main OPC neurons from the indicated temporal windows. Statistical comparisons of synaptic depths between different temporal origins and Notch states were performed using Kruskal-Wallis tests followed by Dunn's post-hoc tests (FSA package), with P-values adjusted using the Bonferroni method (see Supp. Table 1 for one-to-one comparisons between temporal windows).

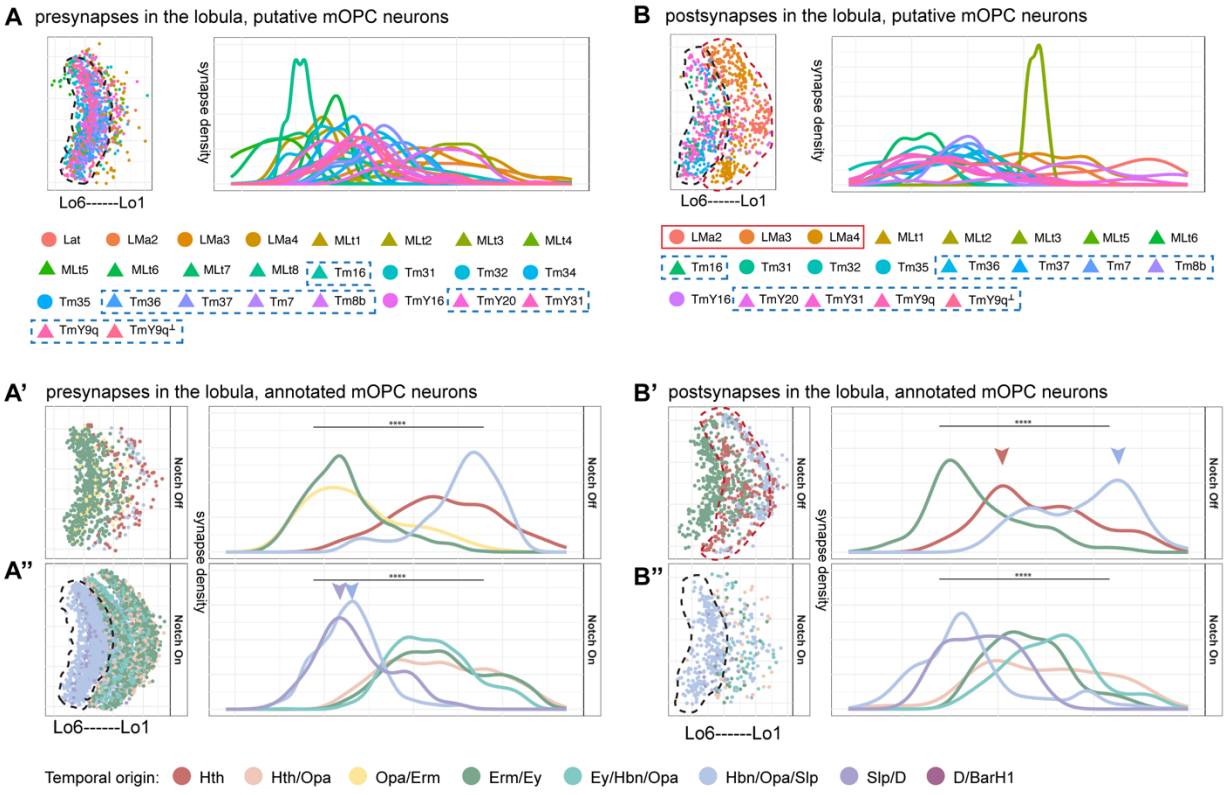

Figure 5. Temporal origin of unannotated main OPC neurons can be inferred from synapse location. **A.** Presynapse distribution in the lobula neuropil of unannotated putative main OPC neurons, color-coded by neuronal type. **B.** Postsynapse distribution in the lobula neuropil of unannotated putative main OPC neurons, color-coded by neuronal type. Notch^{On} neurons are represented as triangles, while Notch^{Off} neurons are represented as circles. Pre- (**A'-A"**) and postsynapse (**B'-B"**) distribution in the lobula neuropil of annotated (previously annotated plus annotated in this work) Notch^{Off} (**A'-B'**) and Notch^{On} (**A"-B"**) main OPC neurons. Synapses are color-coded based on temporal origin, from Konstantinides *et al.*, 2022[11]. Curve graphs indicate synapse density along the lobula neuropil, color-coded by temporal origin. Black dashed outline in the lobula neuropil indicates the neuropil targeting regions of the indicated cholinergic (Notch^{On}) projection neurons (blue dashed rectangles). Red dashed outline in the lobula neuropil indicates the neuropil targeting regions of the indicated GABAergic (Notch^{Off}) neurons (red rectangle).

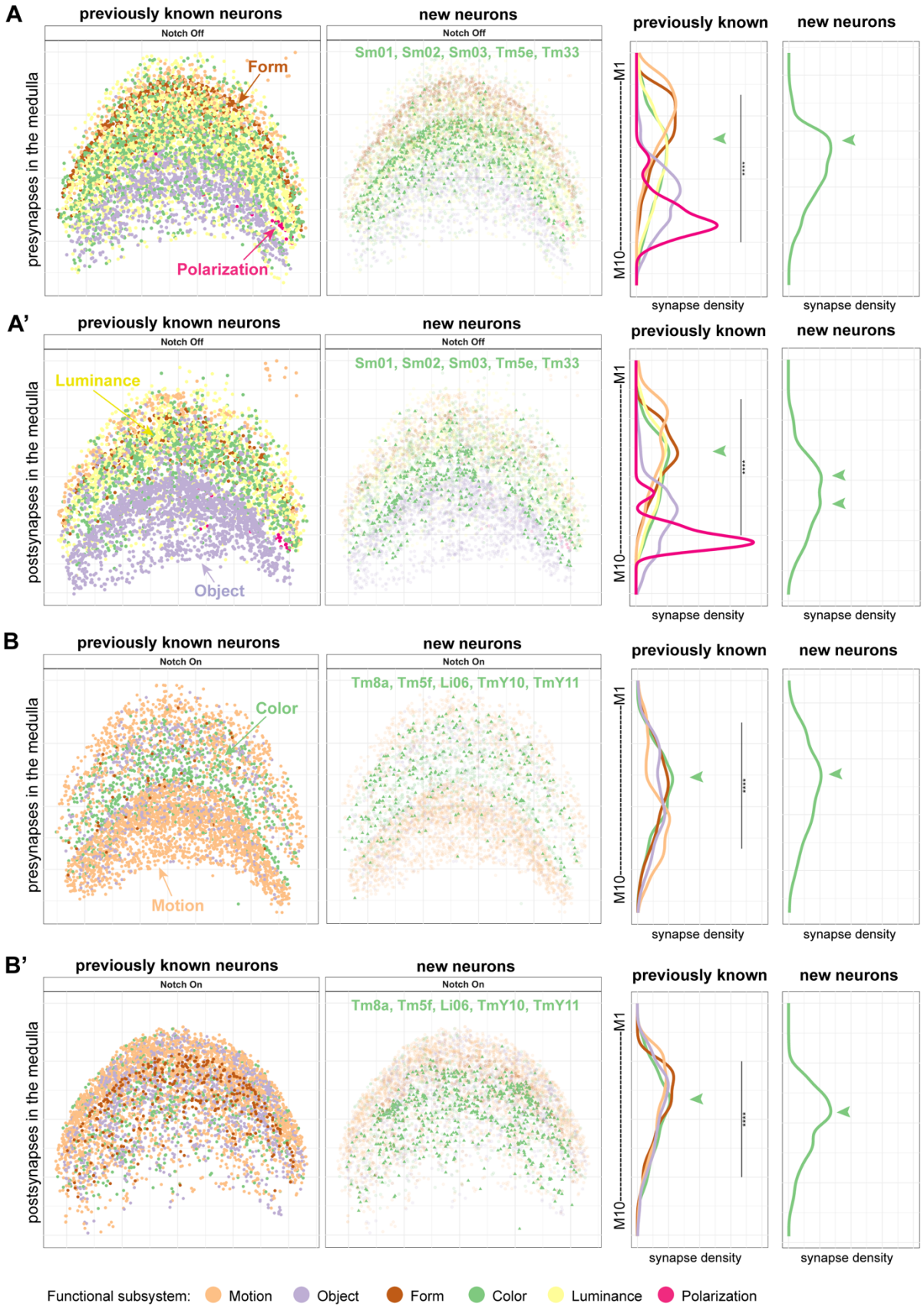

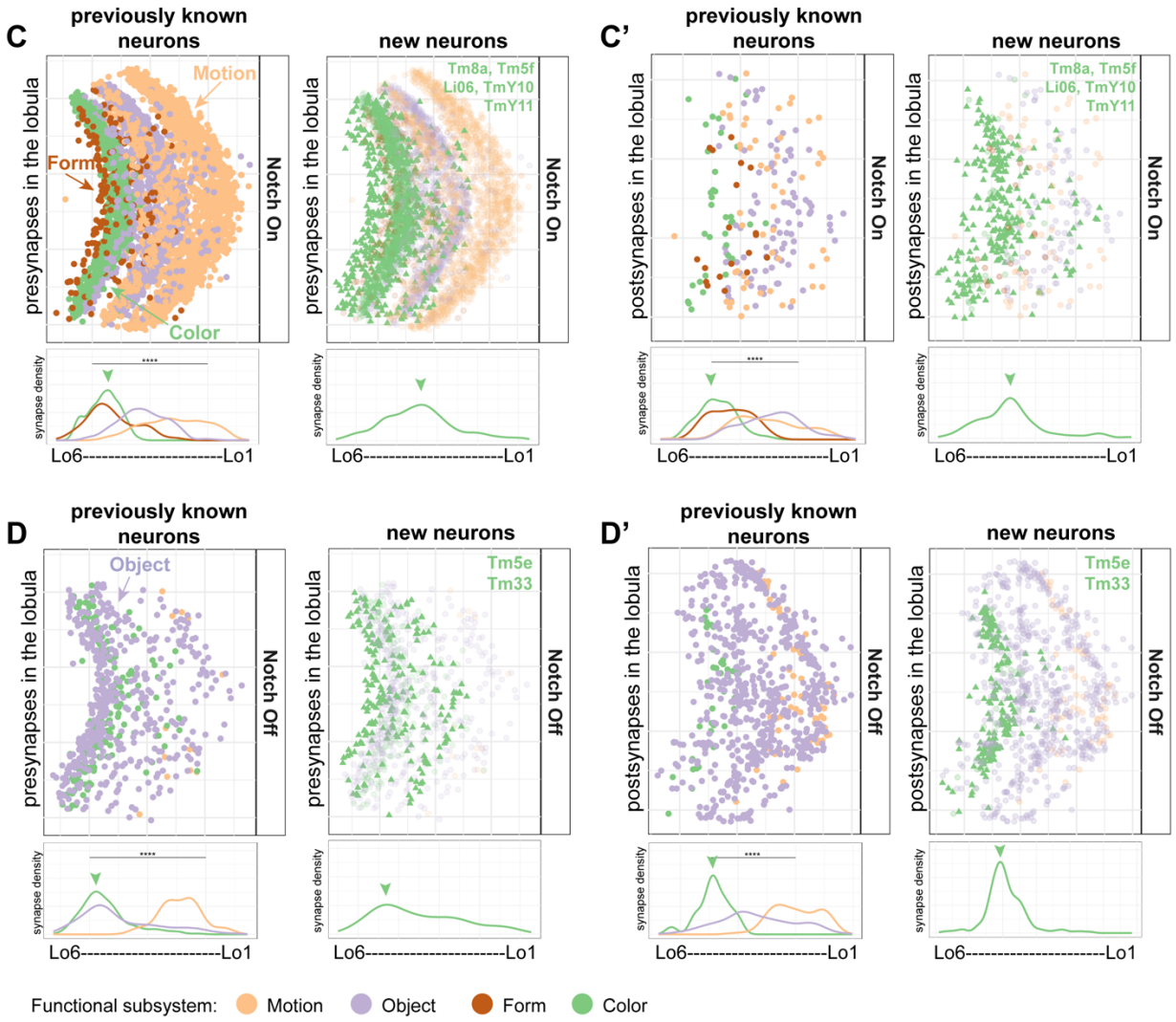

Figure 6. Neuropil targeting of main OPC neurons is associated with specific visual functions.
Comparison between pre- (**A-B**) and postsynapse (**A'-B'**) distribution in the medulla neuropil of both previously annotated and newly annotated Notch^{Off} (**A-A'**) and Notch^{On} (**B-B'**) main OPC neurons. Synapses are color-coded based on predicted functional modality, from Matsliah *et al.*, 2024[30]. Curve graphs indicate synapse density along the neuropil, color-coded by predicted functional modality. Arrowheads indicate peaks of synapse density of main OPC neurons from the Color functional subsystem.
Figure 6 (continuation). Comparison of pre- (**C-D**) and postsynapse (**C'-D'**) distribution in the lobula neuropil of both previously annotated and newly annotated Notch^{On} (**C-C'**) and Notch^{Off} (**D-D'**) main OPC neurons annotated in this work. Synapses are color-coded based on predicted functional modality from Matsliah *et al.*, 2024[30]. Curve graphs indicate synapse density along the neuropil, color-coded by predicted functional modality. Arrowheads indicate peaks of synapse density of main OPC neurons from the Color functional subsystem.
Statistical comparisons of synaptic depths between different functional subsystems were performed using Kruskal-Wallis tests followed by Dunn's post-hoc tests (FSA package), with P-values adjusted using the Bonferroni method (Supp. Table 1).

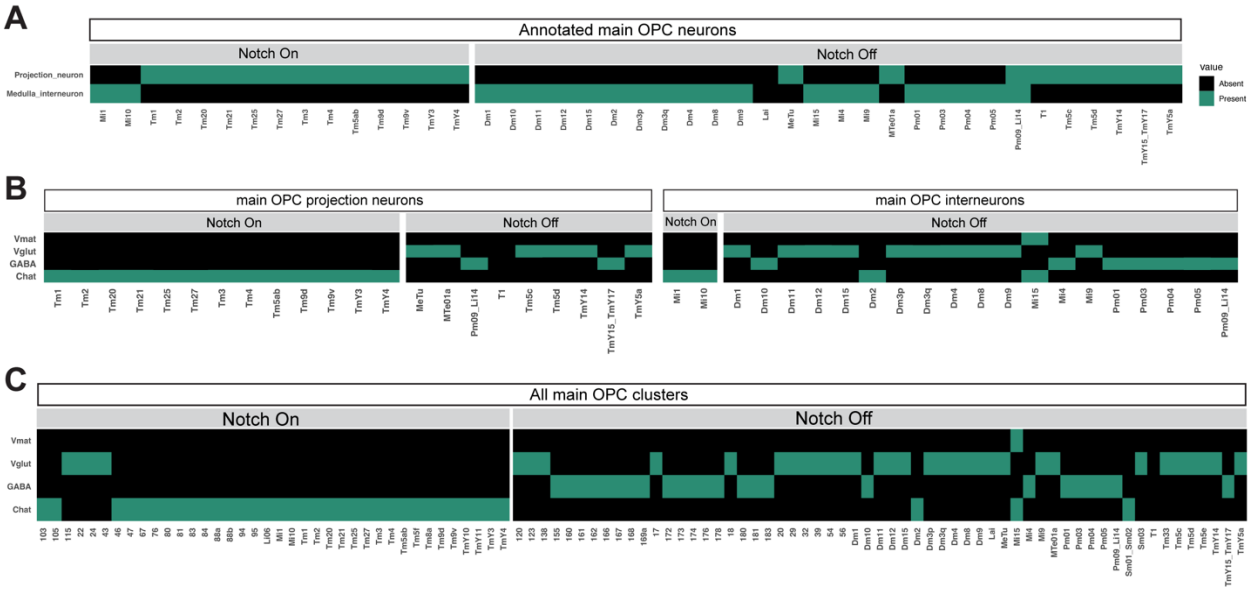

Supp. Figure 1. Relationship between Notch identity and different features of main OPC neurons.
A. Relationship between Notch identity and interneuron or projection neuron classes in the adult for annotated main OPC neurons. All Notch^{On} neurons are projection neurons, except for Mi1 and Mi10. 71% of Notch^{Off} neurons are interneurons, and all the interneurons, except Mi1 and Mi10, are Notch^{Off}.
B. Relationship between Notch identity and neurotransmitter identity in the adult for annotated main OPC classes. All annotated Notch^{On} neurons are cholinergic, independently of whether they are projection neurons or interneurons (Mi1 and Mi10). Only two annotated Notch^{Off} neurons, Dm2 and Mi15, are cholinergic, the rest being either glutamatergic or GABAergic.
C. Relationship between Notch identity and neurotransmitter identity in the adult for annotated and unannotated main OPC neurons. 89% of Notch^{On} clusters are cholinergic (Tm9d and Tm9v are considered one cluster, since they are neuronal subtypes). Only 4 (6.6%) Notch^{Off} neurons are cholinergic, the ones born from the last neuronal temporal window (D/Bar-H1). Mi15 is the only main OPC neuron that expresses Vmat. T1 does not express any of the classical neurotransmitters[30].

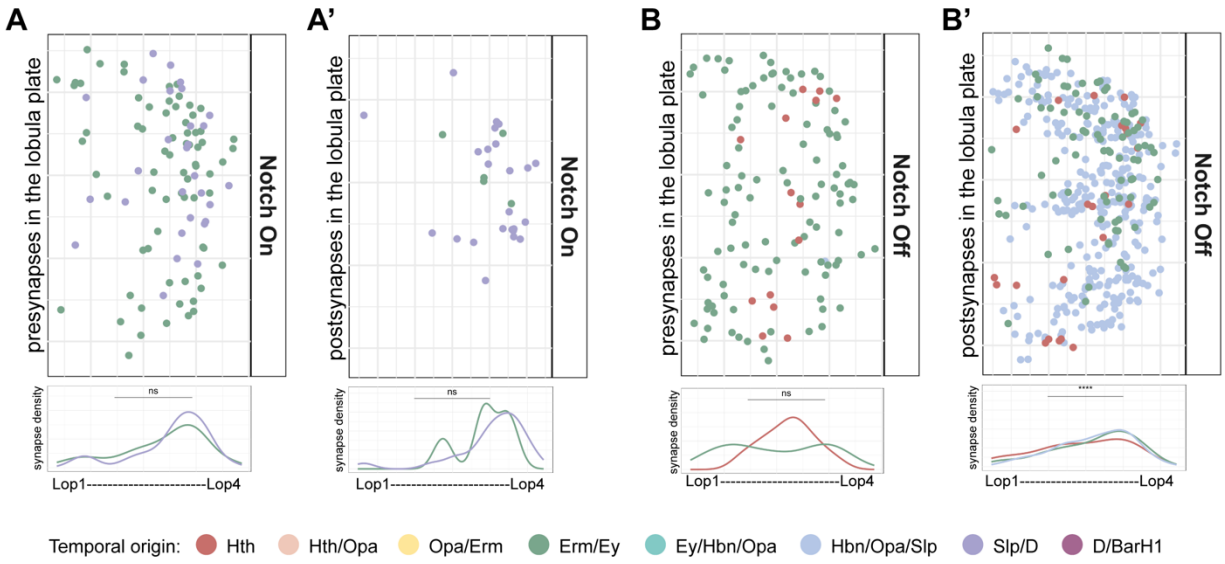

Supp. Figure 2. Synapse location of main OPC neurons in the lobula plate.
Pre- (**A-B**) and postsynapse (**A'-B'**) distribution in the lobula plate neuropil of annotated Notch^{On} (**A-A'**) and Notch^{Off} (**B-B'**) main OPC neurons. Synapses are color-coded based on temporal window of origin, from Konstantinides et al., 2022[11]. Curve graphs indicate synapse density along the neuropil, color-coded by temporal window of origin.
Statistical comparisons of synaptic depths between different temporal origins and Notch states were performed using Kruskal-Wallis tests followed by Dunn's post-hoc tests (FSA package), with P-values adjusted using the Bonferroni method (see Supp. Table 1 for one-to-one comparisons between temporal windows).

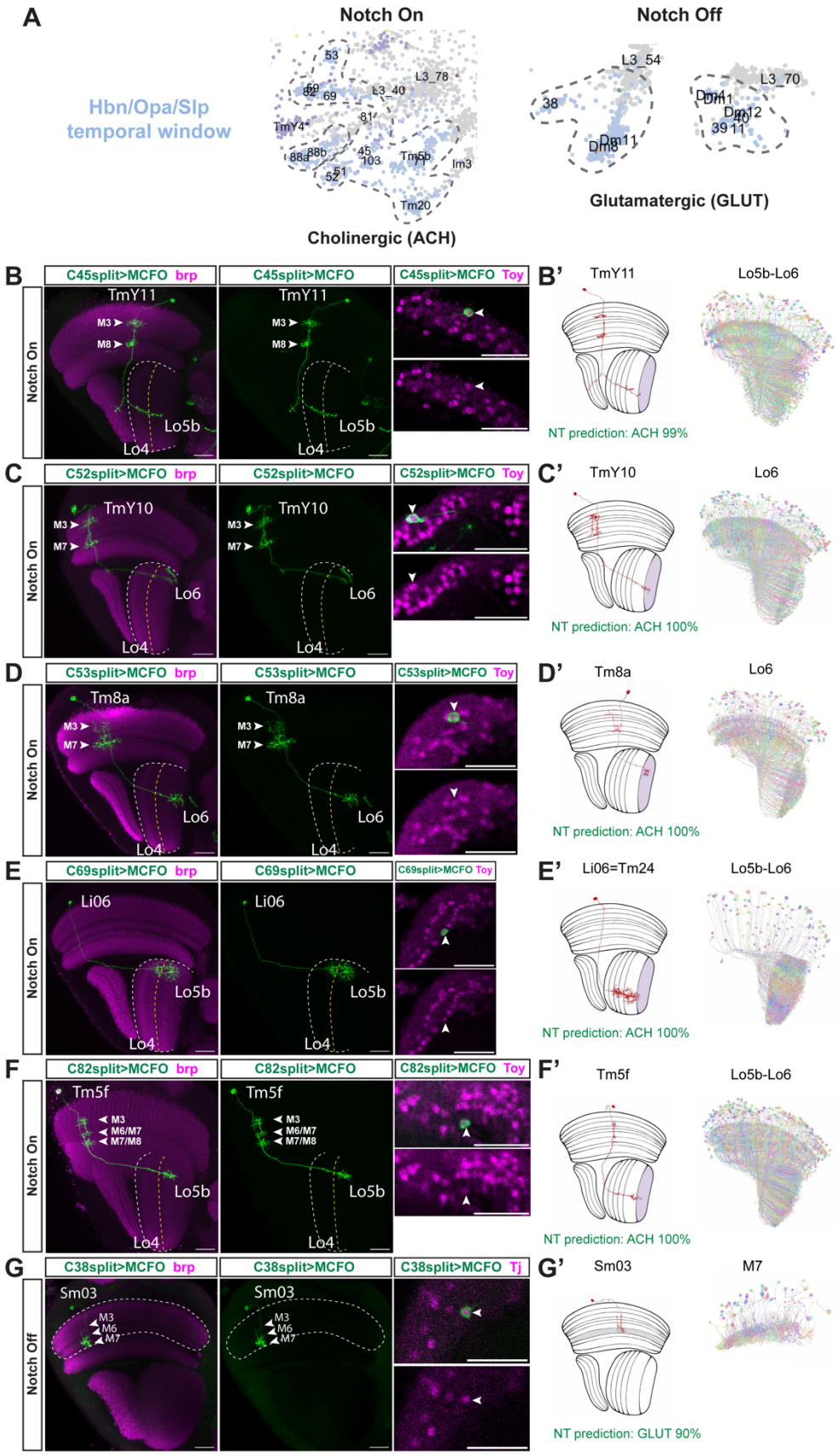

Supp. Figure 3. Characterization of main OPC neurons from the Hbn/Opa/Slp temporal window using sparse labelling.

A. UMAP insets from L3-15h APF scRNA-seq dataset[33] showing the Notch^{On} and Notch^{Off} unannotated clusters from the Hbn/Opa/Slp temporal window and the annotated neurons that cluster close to them.

B-G. Sparse labelling of the indicated split-Gal4 lines, labelling the indicated neurons, and co-staining with either Toy (B-F) or Tj (G). Images are substack projections of segmented single cells from sparse labeling to show distinct morphological features. Anti brp staining is used to visualize the different neuropils. Lo4 layer is indicated with a yellow dashed line. The outline of the lobula and Distal medulla neuropils is indicated with a white dashed line. Medulla (M) and lobula layers (Lo) at which the indicated neurons arborize are indicated. Scale bars: 20 μm.

B'-G'. Left panel. Cartoon depicting the neuronal type from the FlyWire EM dataset[30] matching morphologically the neurons labelled by the indicated split-Gal4 lines and the neurotransmitter (NT) prediction with percentage of accuracy. The lobula layer at which the indicated projection neurons terminate and the medulla layer at which Sm03 terminates are indicated. **Right panel**. Representation of all the neurons from a given EM type from FlyWire dataset[30].

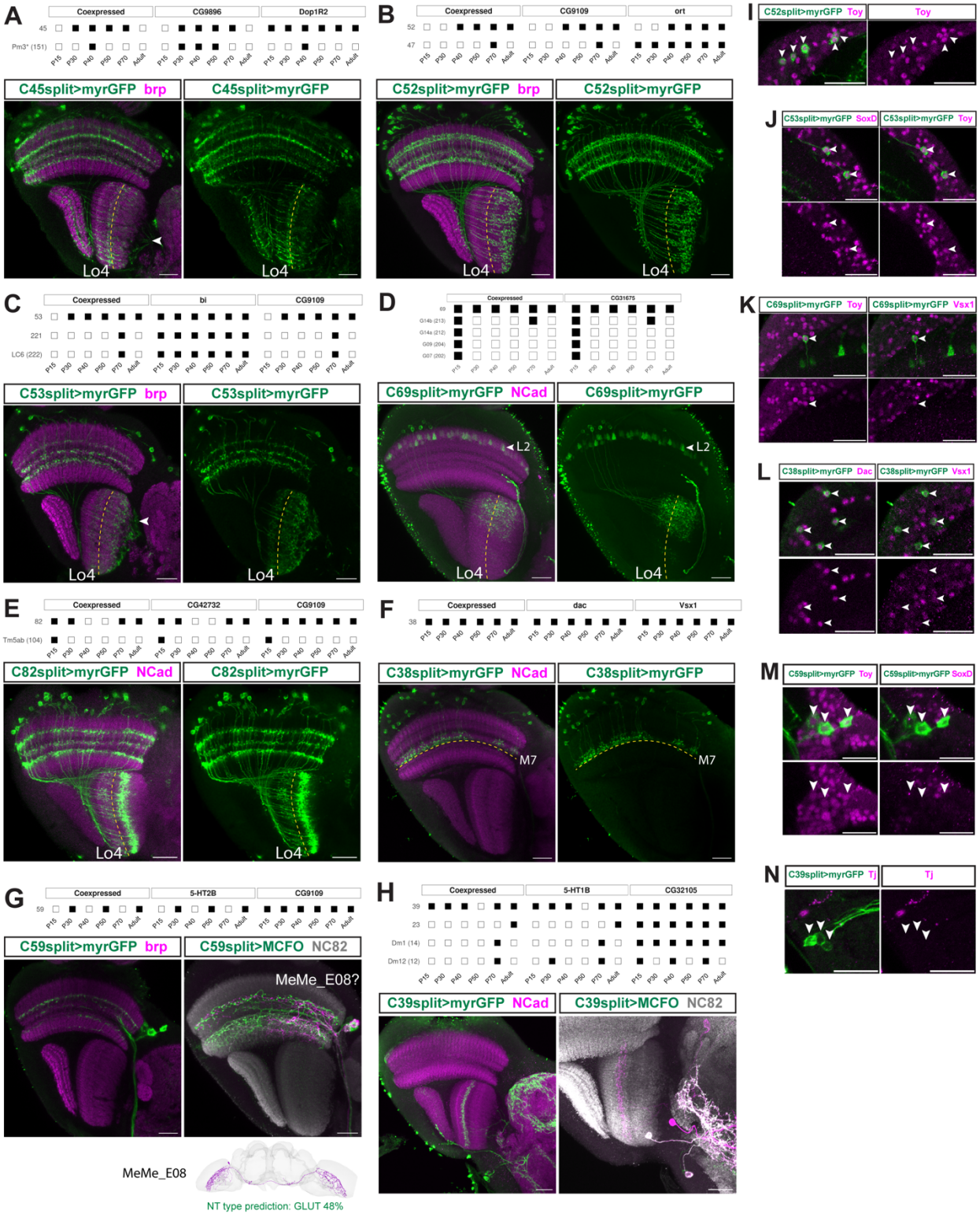

Supp. Figure 4. Characterization of main OPC neurons from the Hbn/Opa/Slp temporal window using GFP and TF expression.

A. Top. Hemidrivers used to specifically label c45. Although this split-Gal4 is not predicted by Mixture Modelling (0.5 threshold)[46] to label c45 in the adult, perdurance from earlier stages (expressed at least at 70h APF, P70) likely allows GFP expression in the adult. **Bottom.** C45 split-Gal4 labels projection neurons (GFP, green) that target both the lobula plate and deep layers of the lobula. **B. Top.** Hemidrivers used to specifically label c52. **Bottom.** C52 split-Gal4 labels projection neurons (GFP, green) that target both lobula plate and deep layers of the lobula. **C. Top.** Hemidrivers used to specifically label c53. **Bottom.** C53 split-Gal4 labels projection neurons (GFP, green) that target deep layers of the lobula. **D. Top.** Hemidrivers used to specifically label c69. **Bottom.** C69 split-Gal4 labels projection neurons (GFP, green) that target deep layers of the lobula. **E. Top.** Hemidrivers used to specifically label c82. **Bottom.** C82 split-Gal4 labels projection neurons (GFP, green) that target deep layers of the lobula. **F. Top.** Hemidrivers used to specifically label c38. **Bottom.** C38 split-Gal4 labels medulla interneurons (GFP, green) that target the serpentine layer (M7). **G. Top.** Hemidrivers used to specifically label c59. **Bottom.** C59 split-Gal4 labels neurons (GFP, green) with big somas located between the medulla cortex and the central brain, which target both the medulla neuropil and the central brain and that are likely not from main OPC origin. These neurons resemble MeMe_E08 from FlyWire[30], which are predicted to be glutamatergic, although with low accuracy (48%). **H. Top.** Hemidrivers used to specifically label c39. **Bottom.** C39 split-Gal4 labels neurons with somas in the central brain (GFP, green) that target the lobula, lobula plate, and central brain and that are likely not from main OPC origin. **I-N.** Immunostaining of the indicated TFs in each cluster.
Neuropils are labelled with brp or NCad (magenta). Lo4 and M7 layers are indicated with a yellow dashed line. Scale bars: 20 μm.

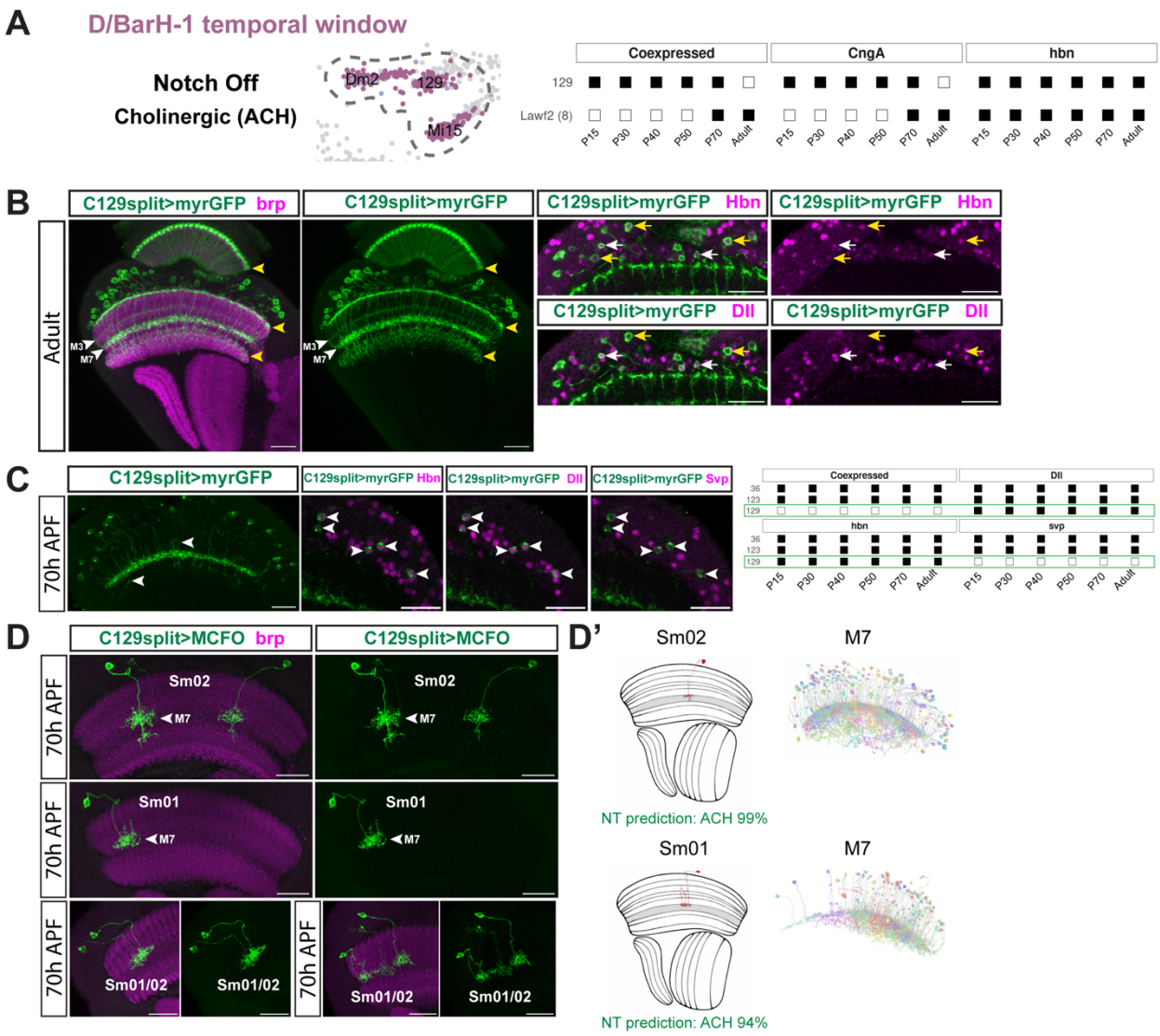

Supp. Figure 5. Characterization of Notch^{Off} neurons that are cholinergic from the D/BarH1 temporal window.

A. Left. UMAP insets from L3-15h APF scRNA-seq dataset[33] showing the unannotated Notch^{Off} cluster 129 and its grouping with Dm2 and Mi15 clusters, from the same D/BarH-1 temporal window. **Right.** Hemidrivers used to specifically label c129. Although CngA-DBD hemidriver is not predicted by Mixture Modelling (0.5 threshold)[46] to label c129 in the adult, perdurance from earlier stages (expressed at least at 70h APF, P70) likely allows GFP expression in the adult. **B.** C129 split-Gal4 driving GFP in the adult. Lawf2, targeting M1, M9, and the lamina (yellow arrowheads), and another neuronal population targeting M3 and M7 are labelled. This line labels at least two neuronal populations, given by the differences in soma size (compare yellow and white arrows) and the presence or absence of Dll expression. **C. Left.** At 70h APF c129 split-Gal4 labels only the Dll-expressing neuronal population, which targets M7 and sometimes sends additional arborizations below M7 and up to M3 (white arrowheads). These neurons are Hbn+, Dll+, and Svp-, confirming that they correspond to c129. **Right.** Developmental expression by Mixture Modelling (0.5 threshold)[46] at the indicated stages of Hbn, Dll, and Svp in c129, c36, and c123. **D.** Sparse labelling of c129 split-Gal4 using MCFO at 70h APF labels Sm01 and Sm02 neurons, as shown by comparison with the FlyWire dataset[30]. **D'. Left**. Morphology of Sm01 and Sm02 neurons in the Flywire dataset and

neurotransmitter (NT) prediction with percentage of accuracy. Medulla layers at which these neurons terminate are colored in grey. **Right**. Medio/Lateral rendering of Sm01 and Sm02 neurons from FlyWire dataset[30], indicating the medulla layer targeted. Neuropils are labelled with brp (magenta). Scale bars: 20 μm.

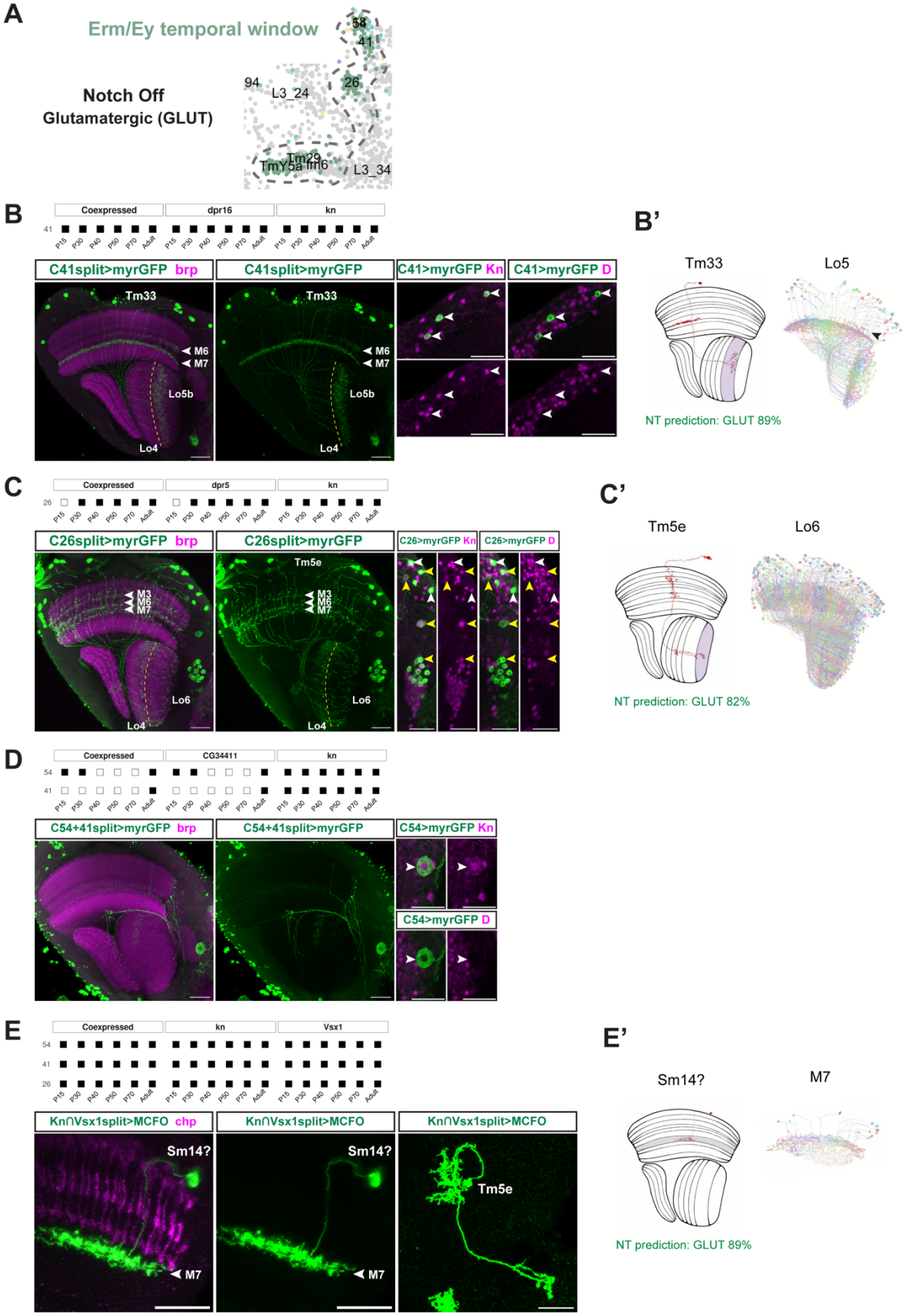

Supp. Figure 6. Characterization of main OPC Notch^{Off} neurons from the Erm/Ey temporal window. **A.** UMAP insets from L3-15h APF scRNA-seq dataset[33] showing the unannotated Notch^{Off} clusters from the Erm/Ey temporal window and the annotated clusters for Tm29 (Tm5d) and TmY5a. **B. Top.** Hemidrivers used to specifically label c41. **Bottom.** C41 split-Gal4 driving GFP, labelling specifically Tm33 neurons, which are Kn+ and D-. **B'. Left.** Morphology of Tm33 neurons in the FlyWire dataset[30] and neurotransmitter (NT) prediction with percentage of accuracy. The lobula layer at which Tm33 terminates is colored. **Right.** Medio/Lateral rendering of Tm33 neurons from FlyWire dataset[30], indicating the lobula layer targeted. Note that not all the neurons have an arborization going up to M6 (black arrowhead). **C. Top.** Hemidrivers used to specifically label c26. **Bottom.** C26 split-Gal4 driving GFP, labelling Tm5e neurons among others. C26 neurons are Kn+ and D+ (white arrowheads, while other neurons labelled by the split-Gal4 line are Kn+ and D- (yellow arrowheads). **C'. Left.** Morphology of Tm5e neurons in the FlyWire dataset and NT prediction with percentage of accuracy. The lobula layer at which Tm5e terminates is colored **Right.** Medio/Lateral rendering of Tm5e neurons from FlyWire dataset[30], indicating the lobula layer targeted. **D. Top.** Hemidrivers used to specifically label c54 and c41 in the adult. **Bottom.** c54+41 split-Gal4 driving GFP, labelling a non-mOPC neuron from the central brain, which is Kn+ and D-. **E. Top.** The split-Gal4 line Kn∩Vsx1 is predicted by Mixture Modelling (0.5 threshold)[46] to specifically label main OPC clusters 54, 41, and 26 at all stages of development. **Bottom.** Sparse labelling of Kn∩Vsx1 split-Gal4 using MCFO labels TmY14, Tm33 (not shown), and neurons that resemble Sm14 and Tm5e, indicating that c54 likely corresponds to Sm14 neurons. **E'. Left.** Morphology of Sm14 neurons in the FlyWire dataset[30] and NT prediction with percentage of accuracy. The medula layer at which Sm14 terminates is colored. **Right.** Medio/Lateral rendering of Sm14 neurons from FlyWire dataset[30], indicating the medulla layer targeted.
Neuropils are labelled with brp, and chaoptin (chp) labels photoreceptors. Lo4 layer is indicated with a yellow dashed line. Scale bars: 20 µm.

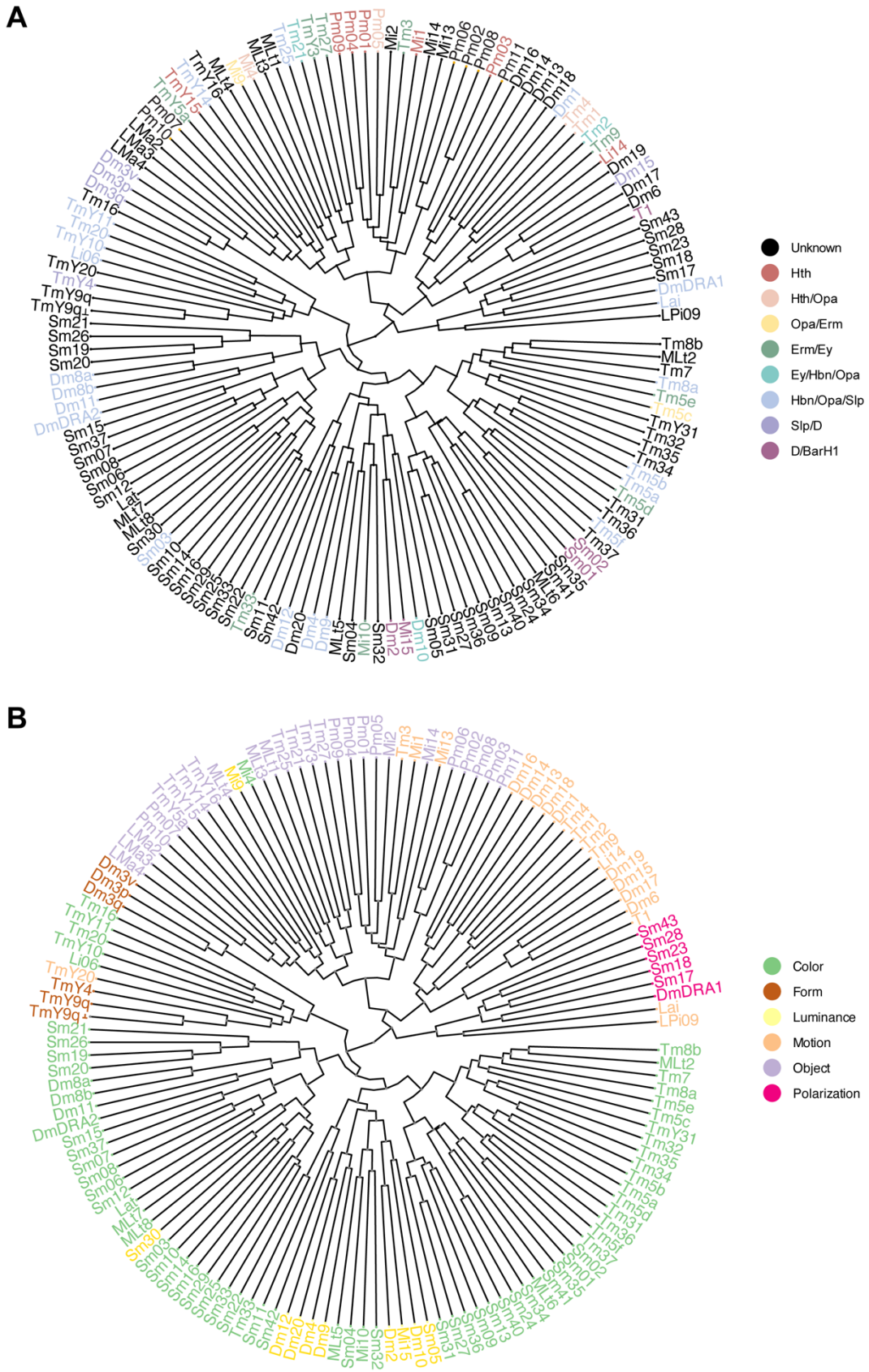

Supp. Figure 7. Similarity tree of all the main OPC neurons based on connectivity from FlyWire.
A. Similarity tree of all the main OPC neurons (annotated plus putative) based on connectivity from FlyWire, color-coded by temporal window of origin[11].
B. Similarity tree of all the main OPC neurons (annotated plus putative) based on connectivity from FlyWire, color-coded by predicted functional subsystem[30].

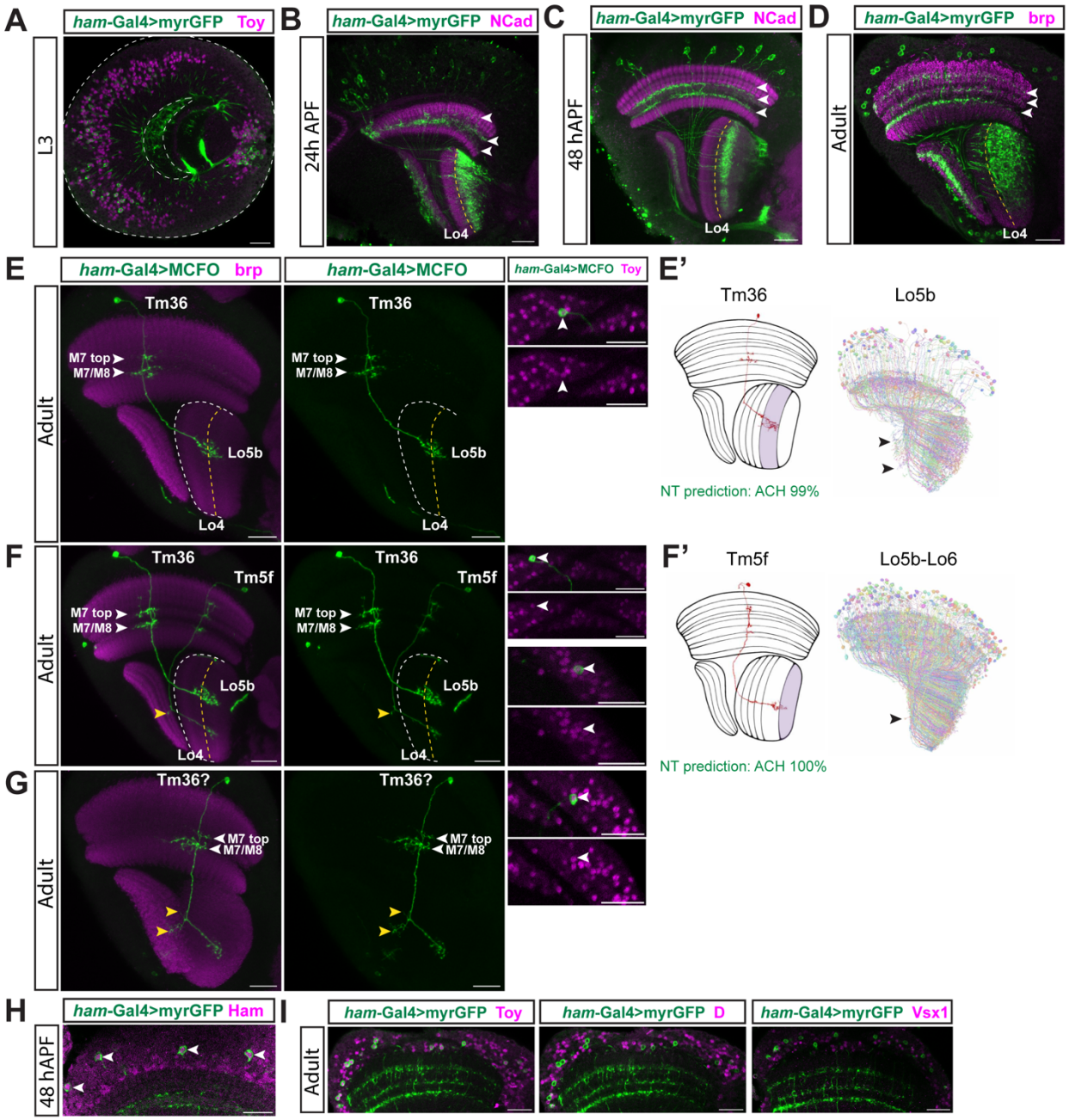

Supp. Figure 8. Sparse labelling of the *Ham*-Gal4 driver line in the adult labels Tm36 neurons.
A-D. *Ham*(R80G09)-Gal4 line driving GFP expression throughout development label projection neurons targeting deep layers of the lobula. White arrowheads indicate neurite targeting in the medulla neuropil. **E-G.** Sparse labelling of Ham-Gal4 in the adult using MCFO labels Tm36 neurons, as shown by comparison with the FlyWire dataset[30] (**E'**). Tm36 was highly variable morphologically, with slightly different dendritic arbors in the medulla (**E-G**) and sometimes with projections to the lobula plate (yellow arrowheads, **G**). Note that some connectomic types assigned to Tm36 identity in FlyWire[30] also have projections to the lobula plate (black arrowheads in **E'**). Tm5f neurons are additionally labelled (**F**) and sometimes had an extra projection to the lobula plate, likely a developmental error (yellow arrowhead in F and black arrowhead in F'). **H.** Neurons labelled by *Ham*-Gal4 are Ham+ at 48h APF. **I.** Neurons labelled by *Ham*-Gal4 in the adult are Toy+, D-, and Vsx1-. Note that clusters that express Ham from the Slp/D window, such as c46 and c94, are D+, while c95 is Vsx1+, and hence c59 is the only remaining Ham+ cluster that could correspond to Tm36 neurons.
Neuropils are labelled with brp or NCad (magenta). Lo4 layer is indicated with a yellow dashed line. The outline of the lobula neuropil is indicated with a white dashed line. Scale bars: 20 µm.

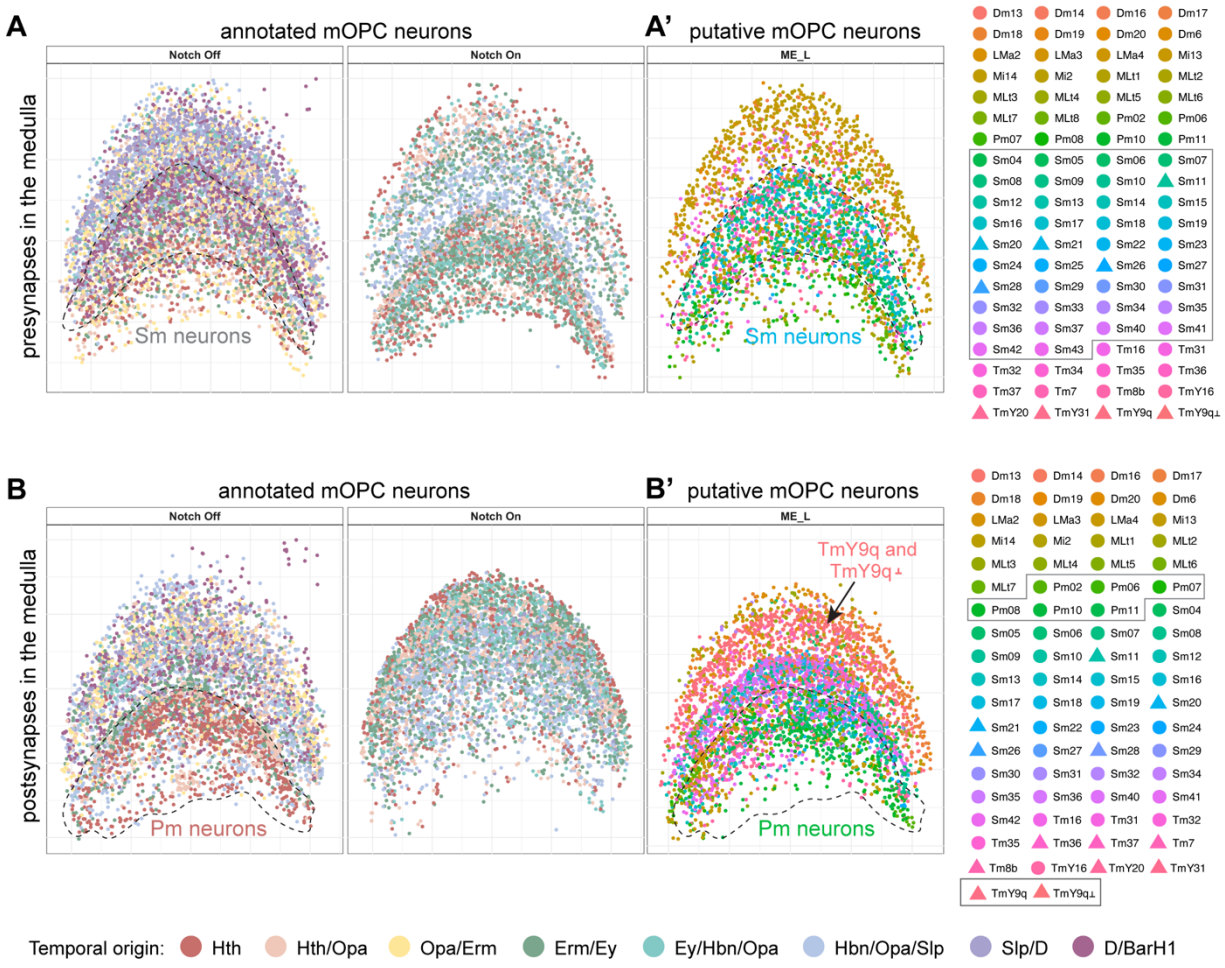

Supp. Figure 9. Temporal origin of unannotated main OPC neurons can be inferred from connectivity: medulla neuropil. Pre- (**A-A'**) and postsynapse (**B-B'**) distribution in the medulla neuropil of annotated (previously annotated plus annotated in this work) Notch^{Off} and Notch^{On} neurons (**A-B**) and putative main OPC neurons (**A'-B'**). Synapses are color-coded based on temporal origin, from Konstantinides et al., 2022[11]. **A"-B".** Curve graphs indicate synapse density of the indicated neurons along the neuropil, color-coded by neuronal type. Black dashed line outline in the medulla indicates the targeting regions of Sm neurons (**A**) and Pm neurons (**B**) (grey rectangles). Preynapse distribution of TmY9 and TmY9⊥ is indicated with an arrow.

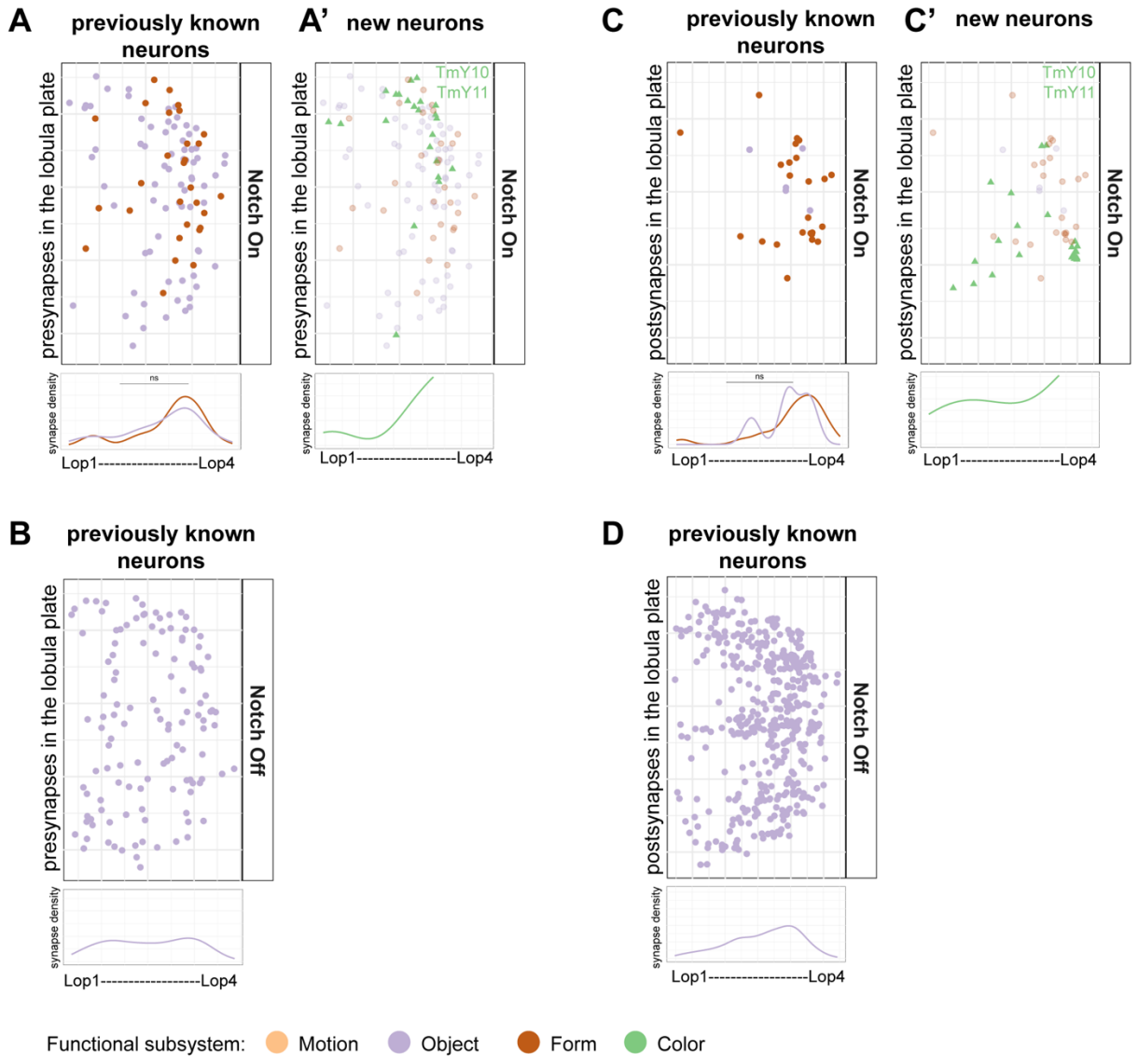

Supp. Figure 10. Synapse distribution of main OPC neurons in the lobula plate, color-coded by functional modality.

Comparison between pre- (**A-A'-B**) and postsynapse (**C-C'-D**) distribution in the lobula plate neuropil of both previously annotated and newly annotated Notch^{On} (**A-A'-C-C'**) and Notch^{Off} (**B-D**) main OPC neurons. There are no newly annotated Notch^{Off} neurons that target the lobula plate. Synapses are color-coded based on predicted functional modality from Matsliah et al., 2024[30]. Curve graphs indicate synapse density along the neuropil, color-coded by predicted functional modality.

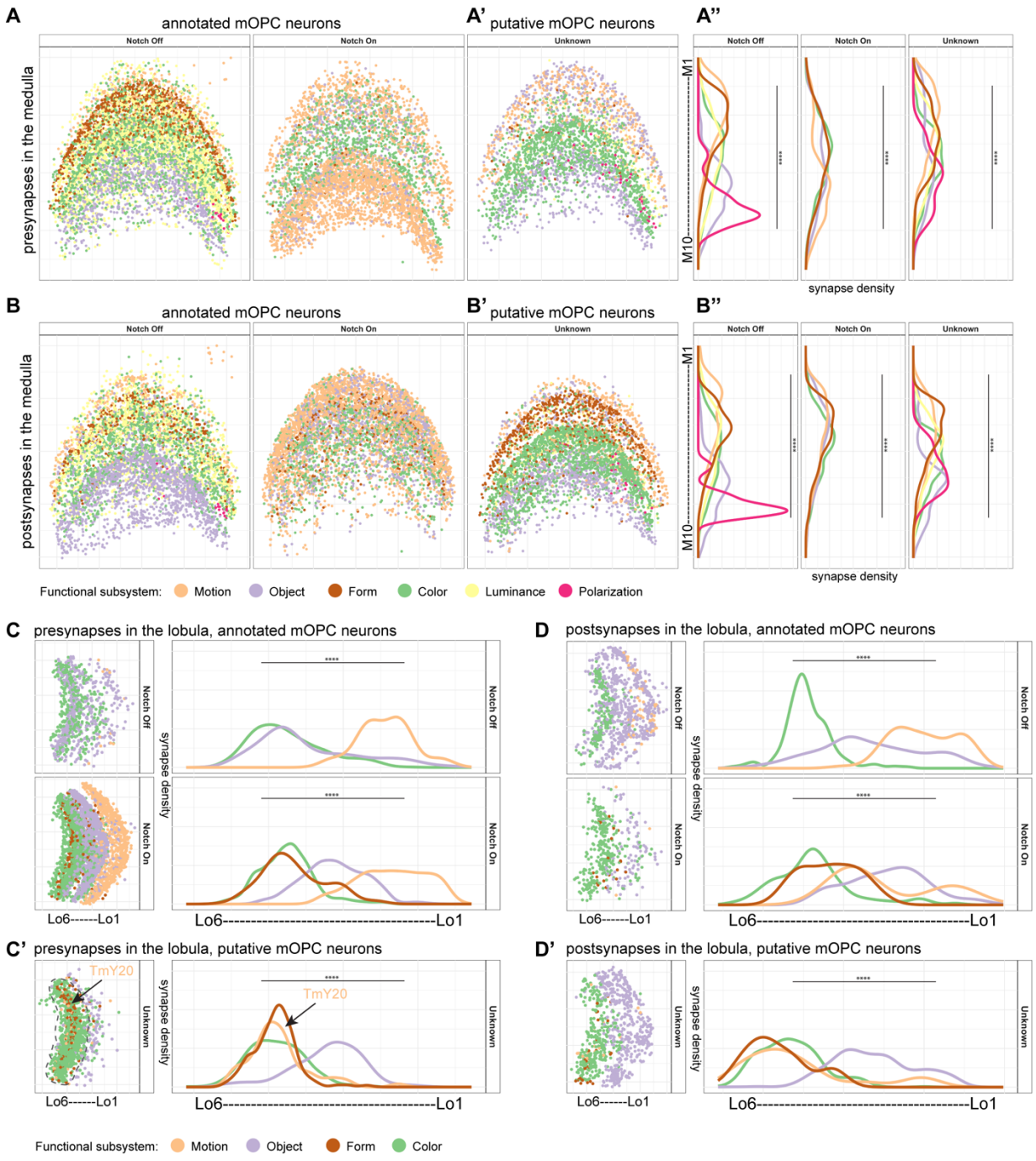

Supp. Figure 11. Synapse distribution of putative main OPC neurons in the medulla and lobula neuropils, color-coded by functional modality.
Pre- (**A-A'**) and postsynapse (**B-B'**) distribution in the medulla neuropil of annotated (previously annotated plus annotated in this work) Notch^{Off} and Notch^{On} neurons (**A-B**) and putative main OPC neurons (**A'-B'**). Synapses are color-coded based on predicted functional modality from Matsliah et al., 2024[30]. Curve graphs indicate synapse density of the indicated neurons along the neuropil, color-coded by predicted functional modality (**A''-B''**).

Pre- (**C-C'**) and postsynapse (**D-D'**) distribution in the lobula neuropil of annotated (previously annotated plus annotated in this work) Notch^{Off} and Notch^{On} neurons (**C-D**) and putative main OPC neurons (**C'-D'**). Synapses are color-coded based on predicted functional modality from Matsliah et al., 2024[30]. Curve graphs indicate synapse density of the indicated neurons along the neuropil, color-coded by predicted functional modality.
Statistical comparisons of synaptic depths between different temporal origins and Notch states were performed using Kruskal-Wallis tests followed by Dunn's post-hoc tests (FSA package), with P-values adjusted using the Bonferroni method (Supp. Table 3).

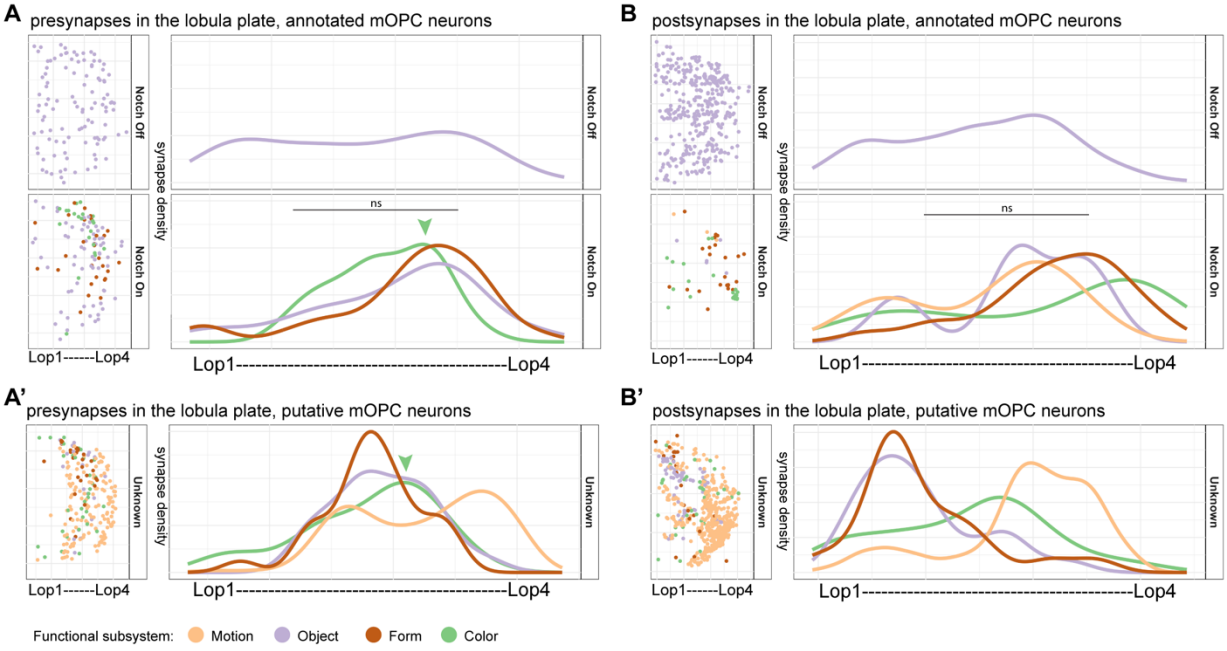

Supp. Figure 12. Synapse distribution of putative main OPC neurons in the lobula plate, color-coded by functional modality.
Pre- (**A-A'**) and postsynapse (**B-B'**) distribution in the lobula plate neuropil of annotated (previously annotated plus annotated in this work) Notch^{Off} and Notch^{On} neurons (**A-B**) and putative main OPC neurons (**A'-B'**). Synapses are color-coded based on predicted functional modality from Matsliah et al., 2024[30]. Curve graphs indicate synapse density of the indicated neurons along the neuropil, color-coded by predicted functional modality. Green arrowheads in A-A' indicate the peak of synaptic density for presynapses of the Color subsystem.
Statistical comparisons of synaptic depths between different temporal origins and Notch states were performed using Kruskal-Wallis tests followed by Dunn's post-hoc tests (FSA package), with P-values adjusted using the Bonferroni method (Supp. Table 3).

Supp. Figure 13. Association between temporal origin and specific functional modalities.
A-F. Bar graphs showing the percentage of main OPC neurons from each of the different functional modalities and Notch status born in each of the indicated temporal windows. Notch^{Off} neurons are represented with a full color pattern, while Notch^{On} neurons are represented with a striped pattern.
G-L. Bar graphs showing the percentage of Notch^{Off} and Notch^{On} neurons from each of the different visual subsystems.
M. Bar graph showing the percentage of main OPC neurons from all the different functional modalities and Notch status born in each of the indicated temporal windows. Notch^{Off} neurons are represented with a full color pattern, while Notch^{On} neurons are represented with a striped pattern.

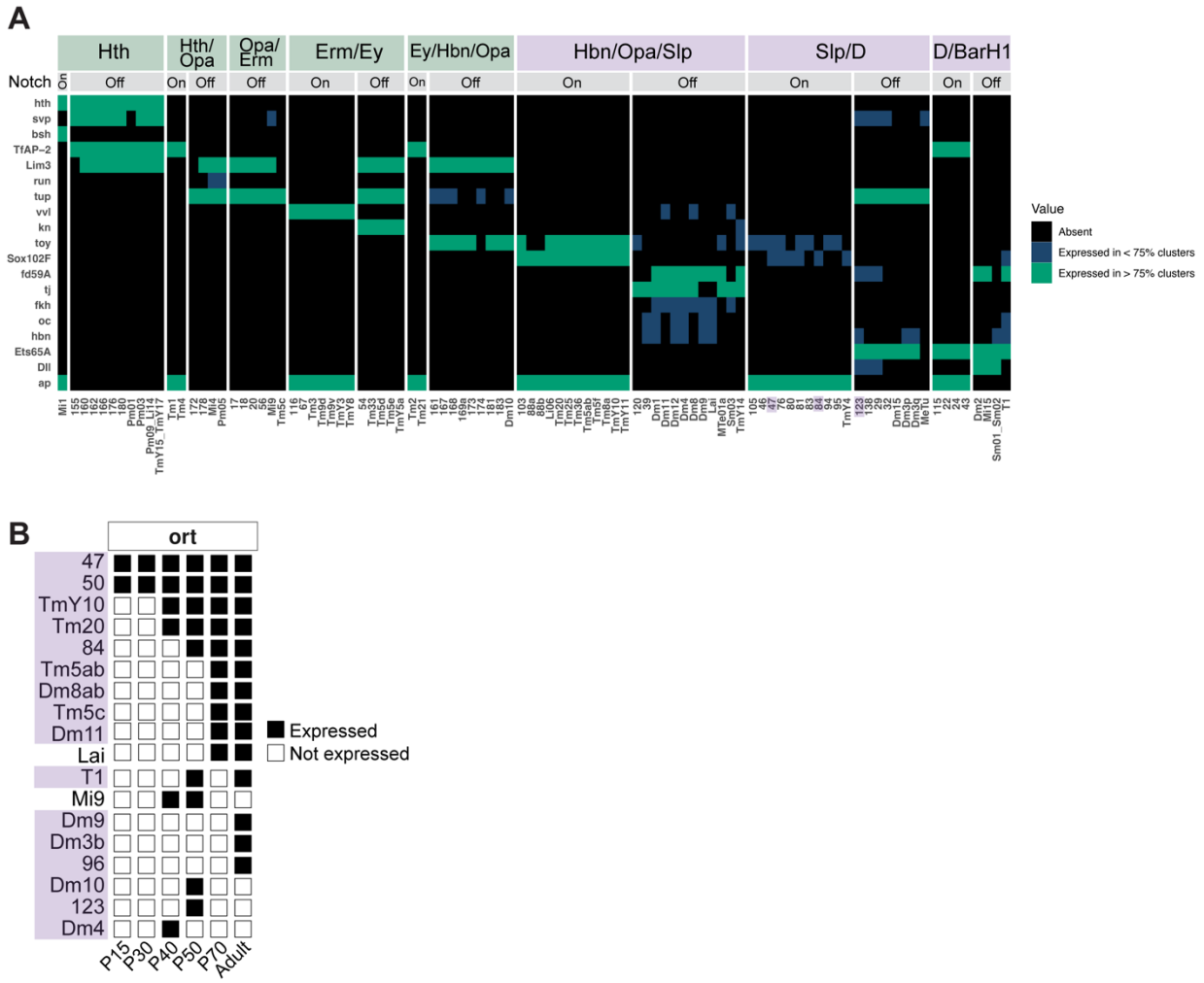

Supp. Figure 14. The TFs used to determine the relative birth order of main OPC neurons are predicted terminal selectors in these neurons. A. Expression in each temporal window of the TFs used to assign the relative birth order of main OPC neurons from Konstantinides *et al.*, 2022[11], at 15h APF. Green: Selectors expressed in more than 75% of the clusters from a given group (temporal window+Notch status). Blue: selectors expressed in less than 75% of the clusters from a given group. Black: absence of expression. **B.** Binarized expression by Mixture Modelling (0.5 threshold)[46] of the histamine receptor ora transientless (ort) throughout development. Ort is expressed in the adult in main OPC neurons that target either deep layers of the lobula (TmY10, Tm20, Tm5ab, Tm5c) or the Distal medulla (Dm neurons and T1).

Sm01

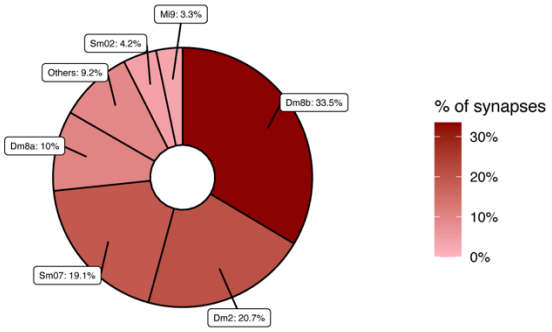

Sm02

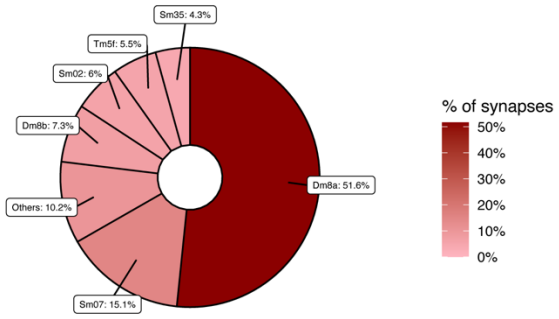

Sm03

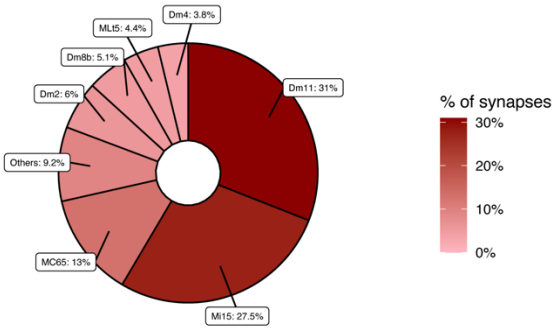

Tm5e

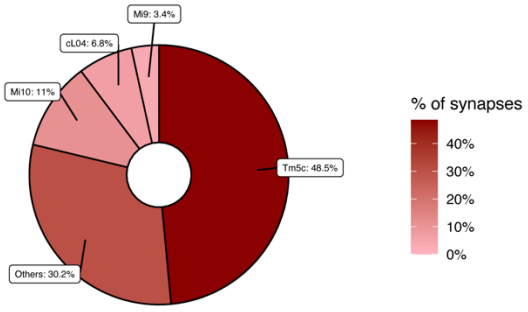

Tm5f

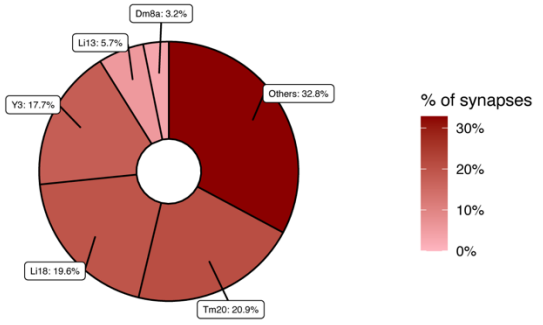

Tm8a

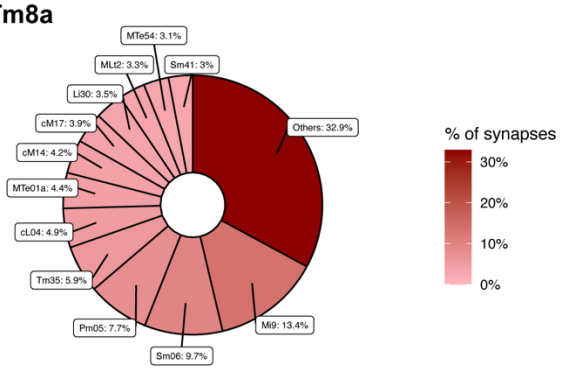

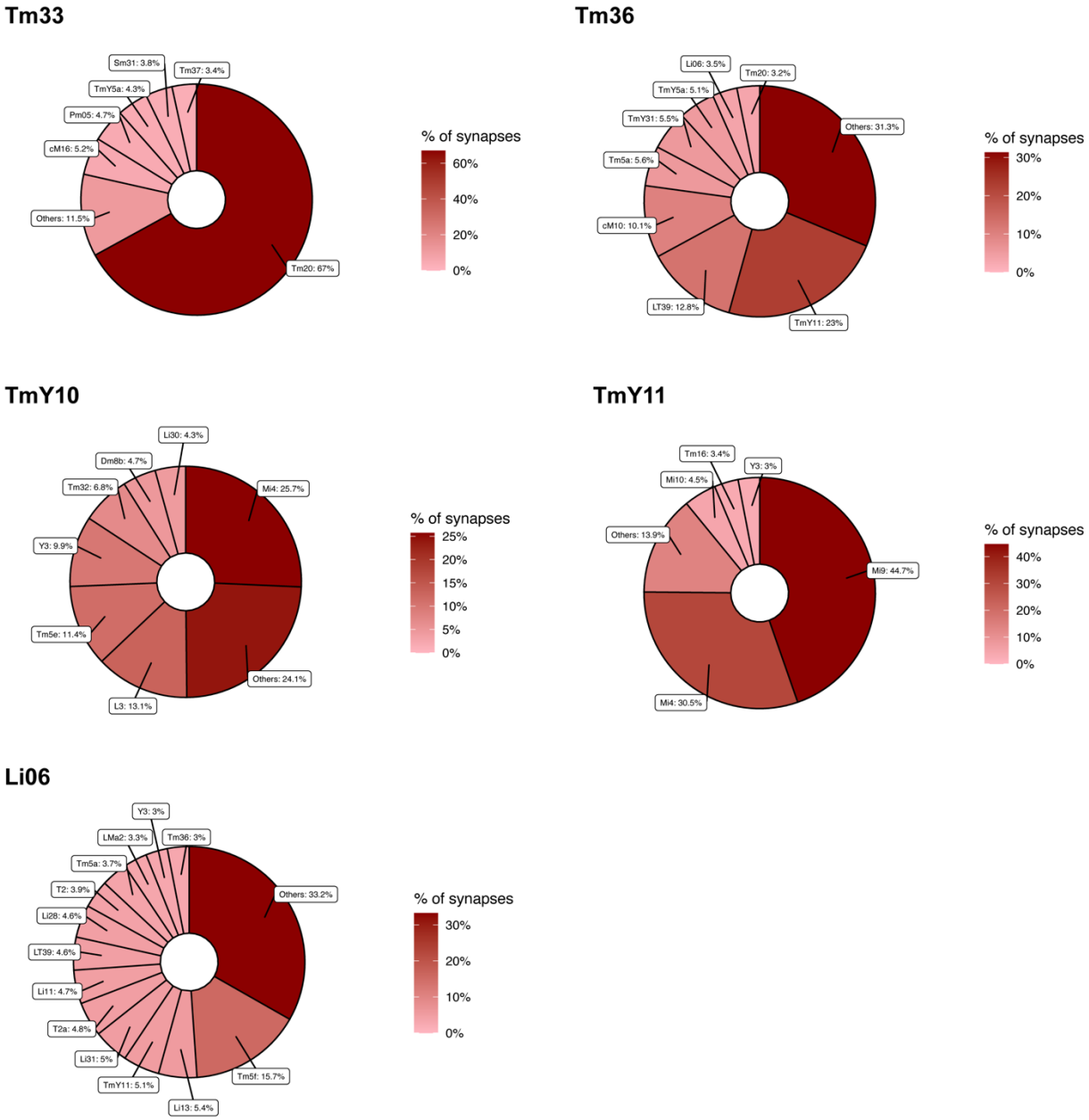

Supp. Figure 15. Donut charts indicating the top synaptic partners of the main OPC neurons identified in this work. Top synaptic partners are ranked by the numbers of synapses per cell type. Neuronal types accounting for less than 3% of the synapses are labelled "Others".

Materials and Methods

Fly strains and fly rearing

Flies were reared on molasses-cornmeal-agar media at 25°C. The fly lines used are described in Supplementary Table 4. Split-Gal4 lines were generated as described in Chen *et al.*,[46] and Li *et al.*,[50]. The R13E12-LexAp65 plasmid was obtained from Janelia[80] and sent to BestGene for injection in the 3rd chromosome (attp2 landing sites). Pupas were staged by selecting white pupa (0h APF) and rearing them at 25°C until the indicated stages for dissection. For sparse labelling using c129 split-Gal4 line, pupa (0h APF) were heat shocked at 38°C for 5min and then reared at 25°C until 70h APF, when they were dissected. For MARCM experiments, L1-L2 larvae were heat shocked for 30 min at 38°C, and then reared at 25°C until flies were dissected in the adult. In all the experiments at least 3 different brains were analyzed.

Antibody generation

A rat polyclonal antibody against Hbn was generated by Genscript using the same epitope as the one in the rabbit anti-Hbn antibody used in Konstantinides *et al.*,[11]:

MMTTTTSQHHQHHPIMPPAMRPAPVQESPVSRPRAVYSIDQILGNQHQIKRSDTPS
EVLITHPHHGHPHHIHHLHSSNSNGSNHLSHQQQQQHSQQQHHSQQQQQQQLQVQAK
REDSPTNTDGGLDVDNDDELSSSLNNGHDLSDMERPRKVRRSRTTFTTFQLHQLERAFE
KTQYPDVFTREDLAMRLDLSEARVQVWFQNRRAKWRKREKFMNQDKAGYLLPEQGLP
EFPLGIPLPPHGLPGHPGSMQSEFWPPHFALHQHFNPAAAAAAGLLPQHLMAPHYKLPN
FHTLLSQYMGLSNLNGIFGAGAAAAAAAASAGYPQNLSLHAGLSAMSQVSPPCSNSSPR
ESPKLVPHPTPPHATPPAGGNGGGGLLTGGLISTAAQSPNSAAGASSNASTPVSVVTKGE
D

Immunohistochemistry

Flies were anesthetized on ice and brains dissected in ice-cold Schneider's media and then transferred to Schneider's media on ice. Larval, 15h APF and adult brains were fixed using 4% paraformaldehyde diluted in PBS 1X for 20 min at room temperature, while fixed 2h on ice for pupal (≥P15) brains. Then, they were rinsed 3 times in 0.5% Triton-X diluted in PBS 1X (PBTx), washed for 30 min in PBTx, and incubated for 30 min in PBTx with 5% goat serum (PBTx-block) at room temperature. They were then incubated at 4°C for 1-2 overnights in primary antibodies diluted in PBTx-block. They were then rinsed 3 times in PBTx, incubated two times for 30 min in PBTx, and incubated at 4°C 1-2 overnights in secondary antibodies diluted in PBTx-block. Finally, they were rinsed 3 times in PBTx, incubated two times for 30 min in PBTx, and mounted in Slowfade before imaging with either a Leica SP8 or Zeiss NLO 980 confocal microscope using a 63x glycerol objective. Image stacks were acquired at 0.8-1 µm optical sections. Images were processed in Fiji and Adobe Illustrator. The antibodies used are described in Supp. Table 4.

Analysis of the FlyWire optic lobe connectome

Data Preprocessing

Connectivity data from the FlyWire database (v783, Oct 2023 release)[30,42] was processed using R (version 4.3.1) with data.table package. Connections between two neurons with more than 5 synapses were considered real and retained for downstream analyses. For all analyses, visualizations were generated using ggplot2 and patchwork packages. The complete analysis pipeline, including all data processing steps and visualization code, is available in Appendix 1.

Raw connectivity data and annotations are available through the FlyWire database[30,42]. In all statistical tests performed (Supp. Tables 1-3), statistical significance levels are denoted as: *p < 0.05, **p < 0.01, ***p < 0.001, ****p < 0.0001, ns: not significant.

Temporal Origin Annotation

Neurons were annotated with their temporal origin (Hth, Hth/Opa, Opa/Erm, Erm/Ey, Ey/Hbn/Opa, Hbn/Opa/Slp, Slp/D, D/BH-1) and Notch status determined by the expression of Ap[7,11,65]. Tm2 and Tm6 (Tm21 in FlyWire) [30,42] were placed in the Ey/Hbn/Opa temporal window after Zhang et al.,[65]. Mi10 and Tm(Y)27 express the TF vvl[44] and although not annotated, are predicted to be born in the Erm/Ey temporal window ($Notch^{On}$ vvl+ neurons), likely corresponding to c67, c70, or c116. TmY8 was not considered as c70 because we realized it had been misannotated in Özel et al.,[33] (the neuron labelled in Extended Data Fig. 4e likely corresponds to Tm27). Moreover, TmY8, which was originally described in Fischbach and Dittrich[29], does not exist in the adult connectome from FlyWire[30,42], indicating that TmY8 might correspond to another neuronal type and had been misannotated as a new neuronal type in Fischbach and Dittrich[29]. TE neurons (clusters 220, 223, 224, and 233) were not included in the analysis because they die during development and hence, they are not present in the adult brain connectome.

Terminal Layer Annotation

To analyze the association between the most remote layer each neuron type projects to in the medulla (M1-M10) and lobula (Lo1-Lo6), we used experimentally validated layer annotations and the FlyWire annotations (https://codex.FlyWire.ai/; Explore > Visual Cell Types Catalog) when experimental data is not available. For visualization, neuronal types were plotted against their temporal origins and annotated terminal layers. Neuron types were plotted with position jittering (width = 0.25, height = 0.1; seed = 2) to prevent overlapping of cell types terminating at the same layer and sharing temporal origin. Neurons were colored by their temporal origin and shaped by their Notch status (On/Off).

Synaptic Depth Analysis

To analyze the distribution of synapses across the depths of each neuropil, we first projected each neuropil using principal component analysis (PCA). Assuming the width and height outsizes the depth of a neuropil, the first and second principal components are expected to capture width and height, with the third component representing the depth. To fulfill the assumption, we selected reference neurons that are 1) abundant and 2) innervate only one layer or adjacent layers. Dm3 was used for the medulla projection, Tm20 (for presynaptic connections) and Tm33 (for postsynaptic connections) were used for the lobula, and T5d was used for the lobula plate. Principal component analysis was performed to capture the anatomical axes, and rotation matrices from the reference cell types were used to project all synaptic coordinates.

We excluded neuronal types that are known to be medulla-intrinsic from the analyses for the lobula and the lobula plate (Mi, Dm, Sm, and Pm neurons). For lobula plate analyses, we only included TmY neurons because it is the only annotated cell class that originates from the OPC and innervates the lobula plate.

Statistical comparisons of synaptic depths between different temporal origins and Notch states were performed as follows: All synapse points passing the filter criteria above were pooled by their cell type label, temporal origin label, or subsystem annotation label. For each identity, the distribution of synaptic points was estimated along the depth axis (PC3) as probability density.

Comparisons were first made using Kruskal-Wallis tests for global differences. If Kruskal-Wallis Test turned out significant ($p < 0.05$), Dunn's post-hoc tests (FSA package) is performed to find pairwise differences, with P-values adjusted using the Bonferroni method. Depth distributions were visualized using ggplot2 (geom_density() for density estimation) and patchwork packages.
To determine the distribution of synapses of all putative main OPC neurons, we included neurons whose somas are in the medulla cortex and are therefore thought to be originated from the main OPC. These neurons were projected to the same PCA space and visualized separately as the Unannotated category and colored by their predicted functional subsystem from FlyWire.

Functional Annotation and Enrichment Analysis

Functional subsystem annotation was retrieved from the FlyWire database (https://codex.FlyWire.ai/; Download Data > Visual Neuron Types). TmY9q__perp is further annotated as a member of the Form subsystem[64]. It is important to note that the method used in Matsliah *et al.*[30,] cannot annotate a neuronal type as belonging to more than one subsystem. Hence, there are specific cases (Mi4, Mi9, Dm9, and Tm25) where neurons were grouped as a different modality as the one described experimentally. For example, the interneuron Mi4 has functionally been identified as part of the ON motion detector[60-61], but it is defined by Matsliah *et al.*[30], to be part of the Color subsystem instead of Motion, since it is considered to be a hub neuron that links motion detection with color vision[30]. Synapse location plots throughout the paper use the functional subsystem annotations from FlyWire. Supp. Fig. 13, however, uses a dual system for functional annotation, considering both FlyWire and previous experimental knowledge[60-62]. In this case, Mi4 is considered to be part of both Motion[60-61] and Color (FlyWire) subsystems, Mi9 was assigned to both Luminance (FlyWire) and Motion[60-61], Dm9 was assigned to both Luminance (FlyWire) and Color, and Tm25 was assigned to both Object (Flywire) and Color[62]. Associations of subsystem annotation and temporal origin were then analyzed using Fisher's exact tests (Supp. Table 3).

Similarity Tree Analysis

To analyze the relationship between the adjacency of temporal origin and the similarity of connectivity and function among neuronal types, we constructed similarity trees based on connectivity and colored them by temporal origins and functional subsystem annotations. Dissimilarity matrix was retrieved from the Source Data of Figure 2 of Matsliah et al.,[30] and was used to calculate Euclidean distance between cell types. Hierarchical clustering was performed (agglomeration method: “complete”) to generate trees which were visualized with ggtree and tidytree packages in R[81].

Analysis of Cell-Type Specific Connectivity Patterns

We analyzed connectivity using two metrics: synaptic count (number of synapses between neuron types) and partner count (number of connected neurons per type). For normalized comparisons, synapse counts were divided by total input or output synapses for each neuron, while connections with neurons with fewer than 20 total synapses were pooled and collectively reported as a sum of “others”.

Consideration of Mi15 as an Sm neuron

Mi15 neurons terminate at medulla layer M7, and hence they do not connect the distal (M1-M6) with the proximal medulla (M8-M10), the requirement described by Fischbach and Dittrich[29] to

be considered a Mi neuron. Hence, Mi15 matches better the Serpentine medulla intrinsic or Sm neurons (termed Cm neurons in Nern et al.,[43]) description and should not be considered an Mi neuron. Moreover, Matsliah et al.,[30] clustered connectomic types of neurons based on shared feature vectors, and Mi15 clustered with most of the Sm neurons, indicating that they are more similar to each other than to Mi neurons.

Matching adult transcriptomic clusters to the FlyWire dataset

We considered cell body location, neuropil targeting, layer-specific arborization patterns and neurotransmitter identity, and compared a given neuron to all the possible cell types within specific neuronal families in FlyWire (e.g., looking at all the possible Tms in the case of using a Tm neuron as a query). Additionally, we checked that the number of cells in the indicated clusters in the adult scRNA-seq dataset[33] matched within a given range to the number of neurons in FlyWire: the number of cells in our adult scRNA-seq dataset corresponds to 2 to 4 times fewer cells in FlyWire. For example, synperiodic or "numerous" neurons (>720 cells in FlyWire) contain the most cells in our scRNA-seq dataset: e.g. Mi1 cluster in the adult scRNA-seq dataset=2298 cells, and Mi1 in FlyWire dataset=796 cells. Less numerous neurons such as Dm12 (109 cells in FlyWire) have accordingly fewer cells in the cluster corresponding to Dm12 in our adult scRNA-seq dataset=283. Heterogeneous clusters are clusters that could contain more than one cell type and are described in Simon et al.,[25].

References

1. Holguera, I. & Desplan, C. Neuronal specification in space and time. *Science* **362**, 176-180, doi:10.1126/science.aas9435 (2018).

2. Sen, S. Q. Generating neural diversity through spatial and temporal patterning. *Semin Cell Dev Biol* **142**, 54-66, doi:10.1016/j.semcdb.2022.06.002 (2023).

3. Erclik, T., Li, X., Courgeon, M., Bertet, C., Chen, Z., Baumert, R., et al. (2017). Integration of temporal and spatial patterning generates neural diversity. Nature 541, 365–370. doi: 10.1038/nature20794.

4. Chen, Y. C. & Konstantinides, N. Integration of Spatial and Temporal Patterning in the Invertebrate and Vertebrate Nervous System. *Front Neurosci* **16**, 854422, doi:10.3389/fnins.2022.854422 (2022).

5. Malin, J. A., Chen, Y. C., Simon, F., Keefer, E. & Desplan, C. Spatial patterning controls neuron numbers in the *Drosophila* visual system. *Dev Cell* **59**, 1132-1145 e1136, doi:10.1016/j.devcel.2024.03.004 (2024).

6. Isshiki, T., Pearson, B., Holbrook, S. & Doe, C. Q. *Drosophila* neuroblasts sequentially express transcription factors which specify the temporal identity of their neuronal progeny. *Cell* **106**, 511-521 (2001).

7. Li, X. *et al.* Temporal patterning of *Drosophila* medulla neuroblasts controls neural fates. *Nature* **498**, 456-462, doi:10.1038/nature12319 (2013).

8. Suzuki, T., Kaido, M., Takayama, R. & Sato, M. A temporal mechanism that produces neuronal diversity in the Drosophila visual center. *Dev Biol* **380**, 12-24, doi:10.1016/j.ydbio.2013.05.002 (2013).

9. Bertet, C. *et al.* Temporal patterning of neuroblasts controls Notch-mediated cell survival through regulation of Hid or Reaper. *Cell* **158**, 1173-1186, doi:10.1016/j.cell.2014.07.045 (2014).

10. Doe, C. Q. Temporal Patterning in the Drosophila CNS. *Annu Rev Cell Dev Biol* **33**, 219-240, doi:10.1146/annurev-cellbio-111315-125210 (2017).

11. Konstantinides, N. *et al.* A complete temporal transcription factor series in the fly visual system. *Nature* **604**, 316-322, doi:10.1038/s41586-022-04564-w (2022).

12. Zhu, H., Zhao, S. D., Ray, A., Zhang, Y. & Li, X. A comprehensive temporal patterning gene network in Drosophila medulla neuroblasts revealed by single-cell RNA sequencing. *Nat Commun* **13**, 1247, doi:10.1038/s41467-022-28915-3 (2022).

13. Ren, Q. *et al.* Stem Cell-Intrinsic, Seven-up-Triggered Temporal Factor Gradients Diversify Intermediate Neural Progenitors. *Curr Biol* **27**, 1303-1313, doi:10.1016/j.cub.2017.03.047 (2017).

14. Syed, M. H., Mark, B. & Doe, C. Q. Steroid hormone induction of temporal gene expression in Drosophila brain neuroblasts generates neuronal and glial diversity. *Elife* **6**, doi:10.7554/eLife.26287 (2017).

15. Cepko, C. Intrinsically different retinal progenitor cells produce specific types of progeny. *Nat Rev Neurosci* **15**, 615-627, doi:10.1038/nrn3767 (2014).

16. Telley, L. *et al.* Temporal patterning of apical progenitors and their daughter neurons in the developing neocortex. *Science* **364**, doi:10.1126/science.aav2522 (2019).

17. Sagner, A. *et al.* A shared transcriptional code orchestrates temporal patterning of the central nervous system. *PLoS Biol* **19**, e3001450, doi:10.1371/journal.pbio.3001450 (2021).

18. Santos-França, P. L., David, L. A., Kassem, F., Meng, X. Q. & Cayouette, M. Time to see: How temporal identity factors specify the developing mammalian retina. *Semin Cell Dev Biol* **142**, 36-42, doi:10.1016/j.semcdb.2022.06.003 (2023).

19. Skeath, J. B. & Doe, C. Q. Sanpodo and Notch act in opposition to Numb to distinguish sibling neuron fates in the Drosophila CNS. *Development* **125**, 1857-1865, doi:10.1242/dev.125.10.1857 (1998).

20. Truman, J. W., Moats, W., Altman, J., Marin, E. C. & Williams, D. W. Role of Notch signaling in establishing the hemilineages of secondary neurons in *Drosophila melanogaster*. *Development* **137**, 53-61, doi:10.1242/dev.041749 (2010).

21. Mark, B. *et al.* A developmental framework linking neurogenesis and circuit formation in the *Drosophila* CNS. *Elife* **10**, doi:10.7554/eLife.67510 (2021).

22. Peng, C. Y. *et al.* Notch and MAML signaling drives Scl-dependent interneuron diversity in the spinal cord. *Neuron* **53**, 813-827, doi:10.1016/j.neuron.2007.02.019 (2007).

23. Zhang, T. *et al.* Generation of excitatory and inhibitory neurons from common progenitors via Notch signaling in the cerebellum. *Cell Rep* **35**, 109208, doi:10.1016/j.celrep.2021.109208 (2021).

24. Engerer, P. *et al.* Notch-mediated re-specification of neuronal identity during central nervous system development. *Curr Biol* **31**, 4870-4878 e4875, doi:10.1016/j.cub.2021.08.049 (2021).

25. Simon, F. *et al.* High-throughput identification of the spatial origins of *Drosophila* optic lobe neurons using single-cell mRNA-sequencing. *bioRxiv*, 2024.2002.2005.578975, doi:10.1101/2024.02.05.578975 (2024).

26. Lacin, H., Zhu, Y., Wilson, B. A. & Skeath, J. B. Transcription factor expression uniquely identifies most postembryonic neuronal lineages in the *Drosophila* thoracic central nervous system. *Development* **141**, 1011-1021, doi:10.1242/dev.102178 (2014).

27. Lacin, H. *et al.* Neurotransmitter identity is acquired in a lineage-restricted manner in the *Drosophila* CNS. *Elife* **8**, doi:10.7554/eLife.43701 (2019).

28. Ngo, K. T., Andrade, I. & Hartenstein, V. Spatio-temporal pattern of neuronal differentiation in the *Drosophila* visual system: A user's guide to the dynamic morphology of the developing optic lobe. *Dev Biol* **428**, 1-24, doi:10.1016/j.ydbio.2017.05.008 (2017).

29. Fischbach, K. F. D. & Dittrich, A. P. The optic lobe of *Drosophila* melanogaster. I. A Golgi analysis of wild-type structure. Cell Tissue Res. 258, 441–475 (1989).

30. Matsliah, A. *et al.* Neuronal parts list and wiring diagram for a visual system. *Nature* **634**, 166-180, doi:10.1038/s41586-024-07981-1 (2024).

31. Konstantinides, N. *et al.* Phenotypic Convergence: Distinct Transcription Factors Regulate Common Terminal Features. *Cell* **174**, 622-635 e613, doi:10.1016/j.cell.2018.05.021 (2018).

32. Kurmangaliyev, Y. Z., Yoo, J., Valdes-Aleman, J., Sanfilippo, P. & Zipursky, S. L. Transcriptional Programs of Circuit Assembly in the *Drosophila* Visual System. *Neuron* **108**, 1045-1057 e1046, doi:10.1016/j.neuron.2020.10.006 (2020).

33. Özel, M. N. *et al.* Neuronal diversity and convergence in a visual system developmental atlas. *Nature* **589**, 88-95, doi:10.1038/s41586-020-2879-3 (2021).

34. Gao, S. *et al.* The neural substrate of spectral preference in *Drosophila*. *Neuron* **60**, 328-342, doi:10.1016/j.neuron.2008.08.010 (2008).

35. Morante, J. & Desplan, C. The color-vision circuit in the medulla of *Drosophila*. *Curr Biol* **18**, 553-565, doi:10.1016/j.cub.2008.02.075 (2008).

36. Nern, A., Pfeiffer, B. D. & Rubin, G. M. Optimized tools for multicolor stochastic labeling reveal diverse stereotyped cell arrangements in the fly visual system. *Proc Natl Acad Sci U S A* **112**, E2967-2976, doi:10.1073/pnas.1506763112 (2015).

37. Huberman, A. D., Clandinin, T. R. & Baier, H. Molecular and cellular mechanisms of lamina-specific axon targeting. *Cold Spring Harb Perspect Biol* **2**, a001743, doi:10.1101/cshperspect.a001743 (2010).

38. Kolodkin, A. L. & Hiesinger, P. R. Wiring visual systems: common and divergent mechanisms and principles. *Curr Opin Neurobiol* **42**, 128-135, doi:10.1016/j.conb.2016.12.006 (2017).

39. Xie, X. *et al.* The laminar organization of the *Drosophila* ellipsoid body is semaphorin-dependent and prevents the formation of ectopic synaptic connections. *Elife* **6**, doi:10.7554/eLife.25328 (2017).

40. de Wit, J. & Ghosh, A. Specification of synaptic connectivity by cell surface interactions. *Nat Rev Neurosci* **17**, 22-35, doi:10.1038/nrn.2015.3 (2016).

41. Sanes, J. R. & Zipursky, S. L. Synaptic Specificity, Recognition Molecules, and Assembly of Neural Circuits. *Cell* **181**, 536-556, doi:10.1016/j.cell.2020.04.008 (2020).

42. Dorkenwald, S. *et al.* Neuronal wiring diagram of an adult brain. *Nature* **634**, 124-138, doi:10.1038/s41586-024-07558-y (2024).

43. Nern, A. *et al.* Connectome-driven neural inventory of a complete visual system. *bioRxiv*, doi:10.1101/2024.04.16.589741 (2024).

44. Hasegawa, E. *et al.* Concentric zones, cell migration and neuronal circuits in the *Drosophila* visual center. *Development* **138**, 983-993, doi:10.1242/dev.058370 (2011).

45. Davis, F. P. *et al.* A genetic, genomic, and computational resource for exploring neural circuit function. *Elife* **9**, doi:10.7554/eLife.50901 (2020).

46. Chen, Y. D. *et al.* Using single-cell RNA sequencing to generate predictive cell-type-specific split-GAL4 reagents throughout development. *Proc Natl Acad Sci U S A* **120**, e2307451120, doi:10.1073/pnas.2307451120 (2023).

47. Lee, T. & Luo, L. Mosaic analysis with a repressible cell marker (MARCM) for *Drosophila* neural development. *Trends Neurosci* **24**, 251-254, doi:10.1016/s0166-2236(00)01791-4 (2001).

48. Schneider-Mizell, C. M. *et al.* Quantitative neuroanatomy for connectomics in *Drosophila*. *Elife* **5**, doi:10.7554/eLife.12059 (2016).

49. Winding, M. *et al.* The connectome of an insect brain. *Science* **379**, eadd9330, doi:10.1126/science.add9330 (2023).

50. Li, S. A., Li, H. G., Shoji, N., Desplan, C. & Chen, Y. D. Protocol for replacing coding intronic MiMIC and CRIMIC lines with T2A-split-GAL4 lines in *Drosophila* using genetic crosses. *STAR Protoc* **4**, 102706, doi:10.1016/j.xpro.2023.102706 (2023).

51. Eckstein, N. *et al.* Neurotransmitter classification from electron microscopy images at synaptic sites in Drosophila melanogaster. *Cell* **187**, 2574-2594 e2523, doi:10.1016/j.cell.2024.03.016 (2024).

52. Apitz, H. & Salecker, I. Spatio-temporal relays control layer identity of direction-selective neuron subtypes in *Drosophila*. *Nat Commun* **9**, 2295, doi:10.1038/s41467-018-04592-z (2018).

53. Pinto-Teixeira, F. *et al.* Development of Concurrent Retinotopic Maps in the Fly Motion Detection Circuit. *Cell* **173**, 485-498 e411, doi:10.1016/j.cell.2018.02.053 (2018).

54. El-Danaf, R. N. *et al.* Morphological and functional convergence of visual projections neurons from diverse neurogenic origins in *Drosophila*. *bioRxiv*, 2024.2004.2001.587522, doi:10.1101/2024.04.01.587522 (2024).

55. Nériec, N. & Desplan, C. From the Eye to the Brain: Development of the *Drosophila* Visual System. *Curr Top Dev Biol* **116**, 247-271, doi:10.1016/bs.ctdb.2015.11.032 (2016).

56. Song, B. M. & Lee, C. H. Toward a Mechanistic Understanding of Color Vision in Insects. *Front Neural Circuits* **12**, 16, doi:10.3389/fncir.2018.00016 (2018).

57. Schnaitmann, C., Pagni, M. & Reiff, D. F. Color vision in insects: insights from *Drosophila*. *J Comp Physiol A Neuroethol Sens Neural Behav Physiol* **206**, 183-198, doi:10.1007/s00359-019-01397-3 (2020).

58. Heath, S. L. *et al.* Circuit Mechanisms Underlying Chromatic Encoding in *Drosophila* Photoreceptors. *Curr Biol* **30**, 264-275 e268, doi:10.1016/j.cub.2019.11.075 (2020).

59. Keles, M. F., Hardcastle, B. J., Stadele, C., Xiao, Q. & Frye, M. A. Inhibitory Interactions and Columnar Inputs to an Object Motion Detector in *Drosophila*. *Cell Rep* **30**, 2115-2124 e2115, doi:10.1016/j.celrep.2020.01.061 (2020).

60. Currier, T. A., Pang, M. M. & Clandinin, T. R. Visual processing in the fly, from photoreceptors to behavior. *Genetics* **224**, doi:10.1093/genetics/iyad064 (2023).

61. Borst, A. & Groschner, L. N. How Flies See Motion. *Annu Rev Neurosci* **46**, 17-37, doi:10.1146/annurev-neuro-080422-111929 (2023).

62. Kind, E. *et al.* Synaptic targets of photoreceptors specialized to detect color and skylight polarization in *Drosophila*. *Elife* **10**, doi:10.7554/eLife.71858 (2021).

63. Shinomiya, K., Nern, A., Meinertzhagen, I. A., Plaza, S. M. & Reiser, M. B. Neuronal circuits integrating visual motion information in *Drosophila melanogaster*. *Curr Biol* **32**, 3529-3544 e3522, doi:10.1016/j.cub.2022.06.061 (2022).

64. Seung, H. S. Predicting visual function by interpreting a neuronal wiring diagram. *Nature* **634**, 113-123, doi:10.1038/s41586-024-07953-5 (2024).

65. Zhang, Y., Lowe, S., Ding, A. Z. & Li, X. Notch-dependent binary fate choice regulates the Netrin pathway to control axon guidance of *Drosophila* visual projection neurons. *Cell Rep* **42**, 112143, doi:10.1016/j.celrep.2023.112143 (2023).

66. Hobert, O. & Kratsios, P. Neuronal identity control by terminal selectors in worms, flies, and chordates. *Curr Opin Neurobiol* **56**, 97-105, doi:10.1016/j.conb.2018.12.006 (2019).

67. Özel, M. N. *et al.* Coordinated control of neuronal differentiation and wiring by sustained transcription factors. *Science* **378**, eadd1884, doi:10.1126/science.add1884 (2022).

68. Schnaitmann, C. *et al.* Color Processing in the Early Visual System of *Drosophila*. *Cell* **172**, 318-330 e318, doi:10.1016/j.cell.2017.12.018 (2018).

69. Wong, K. K. L. *et al.* Origin of wiring specificity in an olfactory map revealed by neuron type-specific, time-lapse imaging of dendrite targeting. *Elife* **12**, doi:10.7554/eLife.85521 (2023).

70. Royce, G. J. Cortical neurons with collateral projections to both the caudate nucleus and the centromedian-parafascicular thalamic complex: a fluorescent retrograde double labeling study in the cat. *Exp Brain Res* **50**, 157-165, doi:10.1007/BF00239179 (1983).

71. Leone, D. P., Srinivasan, K., Chen, B., Alcamo, E. & McConnell, S. K. The determination of projection neuron identity in the developing cerebral cortex. *Curr Opin Neurobiol* **18**, 28-35, doi:10.1016/j.conb.2008.05.006 (2008).

72. Jabaudon, D. Fate and freedom in developing neocortical circuits. *Nat Commun* **8**, 16042, doi:10.1038/ncomms16042 (2017).

73. Di Bella, D. J., Dominguez-Iturza, N., Brown, J. R. & Arlotta, P. Making Ramón y Cajal proud: Development of cell identity and diversity in the cerebral cortex. *Neuron* **112**, 2091-2111, doi:10.1016/j.neuron.2024.04.021 (2024).

74. Osseward, P. J., 2nd *et al.* Conserved genetic signatures parcellate cardinal spinal neuron classes into local and projection subsets. *Science* **372**, 385-393, doi:10.1126/science.abe0690 (2021).

75. Apitz, H. & Salecker, I. A region-specific neurogenesis mode requires migratory progenitors in the *Drosophila* visual system. *Nat Neurosci* **18**, 46-55, doi:10.1038/nn.3896 (2015).

76. Karuppudurai, T. *et al.* A hard-wired glutamatergic circuit pools and relays UV signals to mediate spectral preference in *Drosophila*. *Neuron* **81**, 603-615, doi:10.1016/j.neuron.2013.12.010 (2014).

77. Menon, K. P., Kulkarni, V., Takemura, S. Y., Anaya, M. & Zinn, K. Interactions between Dpr11 and DIP-gamma control selection of amacrine neurons in *Drosophila* color vision circuits. *Elife* **8**, doi:10.7554/eLife.48935 (2019).

78. Courgeon, M. & Desplan, C. Coordination between stochastic and deterministic specification in the *Drosophila* visual system. *Science* **366**, doi:10.1126/science.aay6727 (2019).

79. Christenson, M. P. *et al.* Hue selectivity from recurrent circuitry in *Drosophila*. *Nature Neuroscience* **27**, 1137-1147, doi:10.1038/s41593-024-01640-4 (2024).

80. Jenett, A. *et al.* A GAL4-driver line resource for *Drosophila* neurobiology. *Cell Rep* **2**, 991-1001, doi:10.1016/j.celrep.2012.09.011 (2012).

81. Xu S, Li L, Luo X, Chen M, Tang W, Zhan L, Dai Z, Lam TT, Guan Y, Yu G. 2022. Ggtree: A serialized data object for visualization of a phylogenetic tree and annotation data. *iMeta* 1:e56. doi:10.1002/imt2.56.